TECH LIBRARY KAFB, NM
0061279

NASA CR-1
c.1

NASA CONTRACTOR REPORT

NASA CR-1989

LOAN COPY: RETURN TO
AFWL (DOUL)
KIRTLAND AFB, N. M.

LOCALLY NONSIMILAR SOLUTIONS FOR RADIATING SHOCK LAYER ABOUT SMOOTH AXISYMMETRIC BODIES

by Y. S. Chou

Prepared by
LOCKHEED MISSILES & SPACE COMPANY
Sunnyvale, Calif.
for Ames Research Center

NATIONAL AERONAUTICS AND SPACE ADMINISTRATION • WASHINGTON, D. C. • MARCH 1972

TECH LIBRARY KAFB, NM
0061279

1. Report No.	2. Government Accession No.	3. Recipi...
NASA CR-1989		

4. Title and Subtitle	5. Report Date
"Locally Nonsimilar Solutions for Radiating Shock Layer About Smooth Axisymmetric Bodies"	March 1972
	6. Performing Organization Code
7. Author(s)	8. Performing Organization Report No.
Y. S. Chou	
	10. Work Unit No.
9. Performing Organization Name and Address	11. Contract or Grant No.
Lockheed Missiles & Space Company Sunnyvale, California	NAS 2-5749
	13. Type of Report and Period Covered
12. Sponsoring Agency Name and Address	Contractor Report
National Aeronautics & Space Administration Washington, D.C. 20546	14. Sponsoring Agency Code

15. Supplementary Notes

16. Abstract

Locally nonsimilar solutions for nongray radiating shock layers about smooth axisymmetric bodies have been obtained based on a newly developed approximate method. Good agreement is found with numerical solutions for inviscid cases (both radiating and nonradiating) and with series solutions for the radiating viscous case.

For the inviscid case, the effect of radiative cooling is to destroy the entropy layer; at a distance far from the stagnation point, the shock layer is nearly isothermal. For the viscous case the radiative wall flux approaches that of the inviscid case at a distance far downstream of the stagnation point. The method can also treat surface mass injection.

17. Key Words (Suggested by Author(s))	18. Distribution Statement
Radiation, Shock Layer	UNCLASSIFIED-UNLIMITED

19. Security Classif. (of this report)	20. Security Classif. (of this page)	21. No. of Pages	22. Price*
UNCLASSIFIED	UNCLASSIFIED	59	3.00

*For sale by the National Technical Information Service, Springfield, Virginia 22151

1. Axisymmetric flows
2. Radiation transport theory
3. Shock waves

2 Mar 72

ABSTRACT

Locally nonsimilar solutions for radiating shock layers about smooth axisymmetric bodies have been obtained based on a newly developed approximate method. In this method, nonsimilar terms in the governing equations are defined as dependent variables; model equations are derived for these variables. Solutions based on this method are compared with numerical ones for inviscid cases (both radiating and nonradiating) and compared with a series solution for the radiating viscous case. Agreements were found to be excellent in all the comparisons.

Typical solutions are given for the nongrey radiating shock layer about a body associated with a given axisymmetric shock. It was found that in the inviscid case, the effect of radiative cooling is to destroy the entropy layer; that at a distance far from the stagnation point, the shock layer is nearly isothermal in the inviscid case; and that the radiative wall flux in the viscous case approaches that of the inviscid case at a distance far downstream of the stagnation point.

Solution for a nonradiating case with surface mass injection is also presented to show the feasibility of the present method in handling the mass injection problem.

FOREWORD

This report is one of two volumes covering work performed for the National Aeronautics and Space Administration, Ames Research Center, Moffett Field, California under the terms and specifications of Contract NAS 2-5749. The period of technical performance of the contract was from 10 January 1970 to 7 April 1971. Technical monitor for this contract was Mr. William Page, Hypersonic Free-Flight Branch.

The work carried out under this contract was performed at the Lockheed Palo Alto Research Laboratory, Fluid Mechanics Laboratory, W. C. Marlow, Manager. Principal investigators for this contract were Ken Wilson and Dr. Y. S. Chou.

ACKNOWLEDGMENTS

The author would like to express his sincere appreciation to K. H. Wilson of the Laboratory for his helpful discussions during the course of the work described in this report. Thanks are extended to H. R. Kirch for her contributions in IBM programming, and to M. Frazer for her typing of this manuscript.

NOMENCLATURE

B	blackbody radiation
B_ν	Planck function
c	speed of light
f	u/u_s
f_ξ	$\partial f/\partial \xi$
F	$\beta_1 f f_\xi$
H	total enthalpy, also normalized total enthalpy, normalized by H_s
$\bar{H}_\xi$	$\beta_1 H_\xi$
h	static enthalpy, also normalized static enthalpy, normalized by H_s. Also Planck constant
I_ν	spectral radiation intensity
I_o	integrated intensity
I_i	integrated intensity for band i
$\tilde{k}$	$1 - ky$
k	shock curvature, also Boltzman constant
m	mass
N	mass density viscosity ratio $\rho_s \mu_s / \rho\mu$
N_t	total number density
p	pressure
Pr	Prandtl number
q_w^R	radiative heat flux to the wall
$q_w^R(o)$	radiative heat flux to the wall at stagnation point

$(q_y)_\nu$	spectral radiative heat flux in the direction of y
q_η	normalized radiative heat flux normal to the shock
q_i	normalized radiative heat flux normal to the shock for band i
r	distance measured from axis of symmetry
R_s	shock radius of curvature at stagnation point
Re	Reynolds number $\rho_\infty U_\infty R_s/\mu_{s(o)}$
$\overline{Re}$	effective Raynolds number $\epsilon Re/N$
T	temperature
$T_s(o)$	temperature behind the shock at stagnation point
u	velocity component parallel to the shock
u_∞	free stream velocity
u_s	velocity component parallel to the shock immediately behing the shock
v	velocity component perpendicular to the shock
x	distance parallel to the shock measured from stagnation line
y	distance normal to the shock
z_s	distance along the line of symmetry from the shock stagnation point
μ	viscosity, $\mu_s(o)$ viscosity behind the shock at stagnation point
α_ν	absorption coefficient
α_i	absorption coefficient for band i (Ref. 1)
β_1---β_5	parameters defined by Eq. (15)
Δ	shock layer thickness
ξ	stretched x variable $\xi = \int_o \epsilon\rho_s\mu_s dx$
ϵ	stagnation point density ratio across shock
η	normalized stream function
θ_i	ionization energy

ν frequency

ρ density

ρ_∞ free stream density

τ_i optical depth for band i

ψ stream function

ω parametric variable defined by Eq. (31)

Γ radiative energy parameter $\Gamma = \dfrac{2(kT_s(o))^4}{h^3c^2\rho_\infty u_\infty^2}$

λ_i optical depth for band i defined as $\lambda_1 = \dfrac{6.55 \times 10^{-15} R_s \rho_\infty}{m[kT_s(o)]^3}$

$$\lambda_2 = \lambda_3 = \frac{5.16 \times 10^{-17} \rho_\infty R_s}{m}$$

Γ_i energy parameter associated with band i , defined as $\Gamma_1 = \Gamma\lambda_1$

$\Gamma_2 = \Gamma_3 = \Gamma\lambda_2$

Subscripts

s quantities at shock

o quantities at stagnation line

∞ freestream conditions

w quantities at wall

ξ partial derivative with respect to variable ξ

CONTENTS

Section		Page
	ABSTRACT	i
	FOREWORD	ii
	ACKNOWLEDGMENTS	iii
	NOMENCLATURE	iv
1	INTRODUCTION	1
2	METHOD OF ANALYSIS	4
	2.1 GOVERNING EQUATIONS	4
	2.2 MODEL EQUATIONS FOR NONSIMILAR TERMS IN THE MOMENTUM AND ENERGY EQUATIONS	10
3	METHOD OF SOLUTION	15
	3.1 FORMAL SOLUTION FOR RADIATION FIELD	15
	3.2 INVISCID CASE	16
	3.3 VISCOUS CASE WITHOUT SURFACE MASS INJECTION	18
	3.4 VISCOUS CASE WITH CONSTANT SURFACE MASS INJECTION	20
4	RESULTS	23
	4.1 COMPARISONS WITH EXISTING SOLUTIONS	23
	4.2 TYPICAL SOLUTIONS	34
	4.3 VISCOUS NONRADIATING CASE WITH SURFACE MASS INJECTION	41
5	CONCLUDING REMARKS	45
6	REFERENCES	47
	APPENDIX I - The Thin Shock Layer Approximation and the Maslen's Approximation at the Stagnation Point	49

Section 1

INTRODUCTION

In an early study (Ref. 1), a Blasius type series formulation was employed to obtain the solutions for the thin shock layer flow about a sphere. Due to the limitation of the radius of convergence of the series, the solutions obtained are valid only in the subsonic portion of the nose region. In examining the feasibility of extending the series solution to a distance far from the stagnation point, the series formulation was found to be ineffective. This was due to the slow convergence of the series in predicting the growing of the entropy layer and the difficulties in expanding the absorption coefficients. Recently, Olstad (Ref. 2) obtained the inviscid radiating shock layer solution for a 45° blunted cone by Maslen's method (Ref. 3) of marching along a streamline. This marching scheme, however, cannot readily be applied to the viscous case. Furthermore, in the case of surface mass injection, the inviscid model is too crude even in the stagnation region. To date, therefore, a viscous radiating shock layer solution for a smooth axisymmetric body at distance far downstream from the stagnation region is yet to be obtained, and most importantly, the effect of surface mass injection on the heating distribution far from the stagnation point is not yet quite understood.

In the present study, we will present an approximate method of solution for a thin shock layer about a smooth body, which will be shown to be applicable

to both inviscid and viscous cases with or without surface mass injection. The essence of the present method is to treat the nonsimilar terms in the governing equations as new variables. Model equations are derived for these new variables. A set of coupled differential equations is then obtained and solutions are to be sought locally. This concept of local nonsimilarity has been tested extensively in the boundary layer theory.* A similar method was also developed by Sparrow et al. (Ref. 4) to obtain solutions for two-dimensional incompressible boundary layer flow. The success of this method in treating the boundary layer flow indicates that it may also be successful in treating the shock layer problem, since both the boundary layer equation and the thin shock layer equation are of parabolic type. However, the validity of the method can only be established by comparisons with known correct solutions. In this report, we will include the following comparisons: comparisons with previous series solutions and comparisons with Olstad's numerical solutions for inviscid cases with and without radiative transport.

The present method is an inverse method. Namely, the shock shape is given and the body which supports the given shock is calculated from the mass conservation condition. The method can also be used as a direct method. In this case, an initial shock shape has to be firstly assumed, then iterated on unti a converged shock shape is found. The most attractive aspect of the present method is that the solution is to be sought locally. The original partial differential equation is now treated as a system of ordinary differential equations. Furthermore, the method is quite simple in concept and application.

*Y. S. Chou, unpublished work.

The following assumptions are employed in this study:

(1) Thin shock layer equation is adequate for the description of the flow field.

(2) Quasi-one-dimensional radiative transfer is adequate for the description of radiation field.

(3) The air continuum radiation absorption coefficient can be approximated by a three-band model

(4) The Prandtl number and viscosity density ratio are taken as constant.

(5) The surface mass injection is specified.

(6) The wall is cold so that thermal emission from wall is neglected.

Assumptions (1) and (2) are felt to be essential for the present method. Since, without these assumptions, the full radiating shock layer equations are of elliptic type and there is no previous experience to suggest the validity of the present method in handling an elliptic system. Furthermore, it is felt that for elliptic systems, both upstream and downstream influences will probably not be small; in this case, the application of the locally nonsimilar concept may not be successful. For a radiating shock layer, however, assumption (1) is widely used and believed to be valid. Assumption (2) is shown (Ref. 5) to be sufficiently accurate. Assumption (3) is not essential. One can model the air continuum radiation by more than three bands, but analytic descriptions for each band are necessary for the present method. Assumptions (4) through (6) are used for the purpose of simplicity in computation. They can be readily relaxed.

Section 2
METHOD OF ANALYSIS

2.1 GOVERNING EQUATIONS

The fluid conservation equations for axisymmetric bodies, written in a shock oriented coordinate system (Fig. 1) and valid to order $(\epsilon Re)^{-1}$, are (Ref. 6):

$$\frac{\partial \rho u r}{\partial x} + \frac{\partial \rho v r \tilde{k}}{\partial y} = 0 \tag{1}$$

$$\rho \frac{\partial}{\partial y}\left(\mu \frac{\partial u}{\partial y}\right) - \rho u \frac{\partial u}{\partial x} - \rho v \tilde{k} \frac{\partial u}{\partial y} + \rho k u v - \frac{\partial p}{\partial x} = 0 \tag{2}$$

$$\rho u \frac{\partial v}{\partial x} + \tilde{k} \rho v \frac{\partial v}{\partial y} + k u^2 \rho + \frac{\partial p}{\partial y} = 0 \tag{3}$$

$$\frac{\partial}{\partial y}\left(\frac{\mu}{Pr} + \frac{\partial}{\partial y}\right)\mu\left[\frac{\left(1-\frac{1}{Pr}\right)}{2}\frac{\partial u^2}{\partial y}\right] - \rho u \frac{\partial H}{\partial x} - \tilde{k}\rho v \frac{\partial H}{\partial y} + \int_0^\infty \alpha_\nu \left[\int_0^{4\pi} I_\nu d\Omega - 4\pi B_\nu\right] d\nu = 0 \tag{4}$$

The y momentum equation (Eq. (3)) will be further simplified by retaining only the terms of order unity (see Ref. 6 for order of magnitude analysis). Consequently, Eq. (3) will be replaced by

$$\tilde{k} \frac{\partial p}{\partial y} + k u^2 \rho = 0 \tag{3a}$$

The radiation field is coupled with the fluid mechanics through the integral term in the energy equation, which represents the radiative energy loss or gain per unit volume. In seeking solutions of the radiative transfer equation, we will use the differential approximation. We will also invoke the thin shock layer approximation, namely $\frac{\partial}{\partial x} << \frac{\partial}{\partial y}$. Under these approximations, the

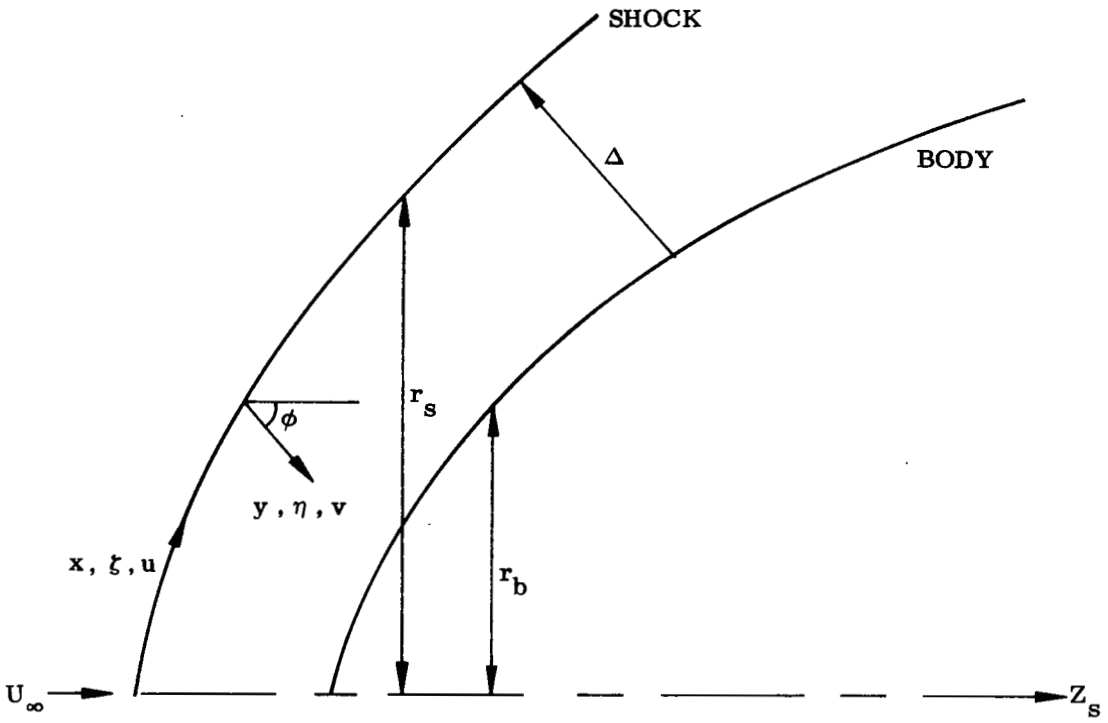

Fig. 1 Sketch of Geometry

integral radiative transfer equation is reduced to the following differential equations:

$$\frac{\partial (q_y)_\nu}{\partial y} = -\alpha_\nu \left[(I_o)_\nu - 4\pi B_\nu \right] \tag{4a}$$

$$\frac{\partial (I_o)_\nu}{\partial y} = -3\alpha_\nu (q_y)_\nu \tag{4b}$$

The validity of Eqs. (4a) and (4b) is discussed in Refs. 1 and 5. The absorption coefficient for air continuum α_ν is modeled by a three-band model. Under this model and after the frequency integration, Eqs. (4a) and (4b) become (in a given band i):

$$\frac{\partial (q_y)_i}{\partial y} = -\alpha_i (I_{o_i} - 4\pi B_i) \tag{5a}$$

$$\frac{\partial (I_o)_i}{\partial y} = -3\alpha_i (q_y)_i \tag{5b}$$

and the radiation integral in energy equation becomes

$$\int_o^\infty \alpha_\nu \left[\int_o^{4\pi} I_\nu d\Omega - 4\pi B_\nu \right] d\nu = \sum_i \alpha_i \left((I_o)_i - 4\pi B_i \right)$$

The detail of the three-band model and the explicit expression of α_i as functions of temperature are given in Ref. 1. Here we will just simply assume that they are known functions of thermodynamics variables.

We now proceed to normalize the variables. The distance x,y and the distance from the axis are normalized by the stagnation point shock radius R_s , the velocity u,v by the freestream velocity u_∞ , the density ρ by the freestream density ρ_∞ , the pressure P by twice the freestream

kinetic pressure $\rho_\infty u_\infty^2$, the shock curvature k by $1/R_s$, the total enthalpy H as well as the static enthalpy h by H_s , the stream function ψ by $\rho_\infty u_\infty R_s^2$, the temperature by the temperature immediately behind the normal shock $T_s(o)$, the viscosity by its value immediately behind the normal shock $\mu_s(o)$, and finally, q_y, I_o, B are all normalized by the quantity $(kT_s(o))^4/h^3c^2$. From here on, the equations are all written in nondimensional form.

We introduce new independent variables ξ and η , defined as

$$\xi(x) = \epsilon\int_o \rho_s\mu_s dx \quad , \quad \eta(x,y) = \frac{\psi}{r_s^2} \quad , \quad d\psi = -\rho ur dy + \rho vr\tilde{k}dx \ .$$

The conservation equations and radiative equations can then be written in ξ,η coordinate as

$$\rho u\left(r_s^2\frac{\partial u}{\partial\xi} - \eta\frac{dr_s^2}{d\xi}\frac{\partial u}{\partial\eta}\right) = -\left(r_s^2\frac{\partial P}{\partial\xi} - \eta\frac{dr_s^2}{d\xi}\frac{\partial P}{\partial\eta}\right) + \frac{N}{\epsilon Re}\rho u\frac{\partial}{\partial\eta}\left(u\frac{\partial u}{\partial\eta}\right) \qquad (6)$$

$$\frac{\partial P}{\partial\eta} = kur_s \qquad (7)$$

$$\epsilon\rho_s\mu_s\left[r_s^2\frac{\partial H}{\partial\xi} - \eta\frac{dr_s^2}{d\xi}\frac{\partial H}{\partial\eta} - \frac{N}{\epsilon Re}Pr\left(u\frac{\partial H}{\partial\eta}\right) - \frac{N}{\epsilon Re}\left(1-\frac{1}{Pr}\right)\frac{\partial}{o\eta}\left(u^2\frac{\partial u}{\partial\eta}\right)\right] = -r_s\sum_i\frac{\Gamma_i}{\lambda_i}\frac{\partial(q_\eta)_i}{\partial\eta}$$

$$u\frac{\partial(q_\eta)_i}{\partial\eta} = -\lambda_i r_s\alpha_i[(I_o)_i - 4\pi B_i] \qquad (9)$$

$$u\frac{\partial(I_o)_i}{\partial\eta} = -3\lambda_i r_s\alpha_i(q_\eta)_i \qquad (10)$$

with $i = i,2,3$ and $Re = \rho_\infty u_\infty R_s/\mu_s(o)$. In arriving at Eqs. (6) through (8), the approximations $r \approx r_s$, $\tilde{k} = 1$ and $\rho\mu/\rho_s\mu_s = N$ = constant were made.

Expressions for radiation parameters λ_i and Γ_i (these are constants for given body size and freestream conditions) are given in Ref. 1. For the sake of simplicity, from here on we will write $q_i = (q_\eta)_i$, $I_i = (I_o)_i$ and $\overline{Re} = \frac{\epsilon Re}{N}$. A detailed discussion on the equations of state is also given in Ref. 1. We simply list the state equations as follows

$$\frac{P}{P_s} = \frac{\rho}{\rho_s} \left(\frac{h}{h_s}\right)^{0.84} \tag{11}$$

$$T = \left(\frac{P}{\epsilon\rho}\right)^{\frac{1}{1.72}} \tag{12}$$

Now Eqs. (6) through (12) are to be solved by satisfying the proper boundary conditions. The boundary conditions for the flow field are given as follows:

At the shock

$$\eta = \tfrac{1}{2}\ ,\ u = u_s\ ,\ P = P_s\ ,\ H = H_s \quad \text{and} \quad I_i - 2q_i = 0 \quad \text{for all} \quad i\ ;$$

At the body

$$\eta = \eta_w\ ,\ u = 0\ ,\ H = H_w \quad \text{and} \quad I_i + 2q_i = 0 \quad \text{for all } i$$

where u_s, H_s, P_s, ρ_s are given by oblique shock relations. In these boundary conditions, we have assumed that the gas ahead of the shock and the body are cold so that there is no thermal emission. We also note that the boundary condition at body includes the surface mass injection, i.e., $\eta_w \neq 0$ in general.

In order to simplify the computation further, we replace the right hand side of Eq. (7) by its value at shock. This is generally referred to as Maslen's approximation (Ref. 3). This approximation is believed to be not valid in the stagnation region (Ref. 7). In the appendix, however, we will show that this approximation is consistent with the thin shock layer approximation. Under this approximation, the pressure field is given by

$$P = P_s + (\eta - \tfrac{1}{2}) k_s u_s r_s \tag{13}$$

Let us now define $f = \frac{u}{u_s}$. After using Eq. (13) one can obtain an equation for f from Eq. (6). We then write down the final form of the x-momentum equation as follows

$$\frac{f}{2}\frac{\partial^2 f^2}{\partial \eta^2} + \bar{R}e\beta_5 \left[\eta \frac{\partial f^2}{\partial \eta} - \frac{\beta_1}{2}(f_\xi^2) - \beta_2(f^2 - \frac{2}{\rho}) + \frac{1}{\rho}(\beta_4 - \eta\beta_3) \right] = 0 \tag{14}$$

where $f_\xi^2 = \frac{\partial f^2}{\partial \xi}$ and β_1 to β_5 are parameters. These are defined as

$$\beta_1 = r_s / \frac{dr_s}{d\xi}$$

$$\beta_2 = \frac{\beta_1}{u_s}\frac{du_s}{d\xi}$$

$$\beta_3 = \frac{r_s k_s}{u_s}(\beta_2 - 1) + \beta_1 \frac{r_s}{u_s}\frac{dk_s}{d\xi} \tag{15}$$

$$\beta_4 = \frac{\beta_3}{2} + \frac{k_s r_s}{u_s}$$

$$\beta_5 = \frac{r_s}{u_s}\frac{dr_s}{d\xi}$$

We note that all the β's are functions of shock shape alone. Hence, for an inverse problem, β's are all given parameters. The boundary condition for f is simply $f = 1$ at the shock, and $f = 0$ (no slip) at the wall. Similarly, the energy equation can be rewritten as follows

$$\frac{\partial}{\partial \eta}\left(f \frac{\partial H}{\partial \eta}\right) + u_s^2 (Pr - 1)\frac{\partial}{\partial \eta}\left(f^2 \frac{\partial f}{\partial \eta}\right) + \bar{R}ePr\beta_5 \left[2\eta \frac{\partial H}{\partial \eta} - \beta_1 H_\xi - \frac{\beta_1}{\epsilon \rho_s \mu_s r_s} \sum_i \frac{\Gamma_i}{\lambda_i}\frac{\partial q_i}{\partial \eta} \right] = 0 \tag{16}$$

where $H_\xi = \frac{\partial H}{\partial \xi}$

The system of equations to be solved are thus Eqs. (9), (10), (11), (12), (14) and (16). One immediately observes from Eqs. (14) and (16) that the only nonsimilar terms which prevent the existence of local solutions are f_ξ^2 and H_ξ (we note because of the quase-one dimensional radiative transfer approximation, the radiative transfer equations, Eqs. (9) and (10), are essentially locally similar).

2.2 MODEL EQUATIONS FOR NONSIMILAR TERMS IN THE MOMENTUM AND ENERGY EQUATIONS

We will now define $\beta_1 f_\xi^2$ and $H_\xi \beta_1$ as new variables. We proceed to derive model equations for $\beta_1 f_\xi^2$ and $\beta_1 H_\xi$. Let us first consider $\beta_1 f_\xi^2$. One obvious way to obtain an equation for $\beta_1 f_\xi^2$ is by differentiating Eq. (14) with respect to ξ and multiplying the resulting equation by β_1. We obtain

$$\frac{F}{2f}\frac{\partial^2 f}{\partial \eta^2} + f\frac{\partial^2 F}{\partial \eta^2} + 2\bar{R}e\beta_5\eta\frac{\partial F}{\partial \eta} = \frac{\beta_{5\xi}}{2\beta_5}\beta_1 f\frac{\partial^2 f^2}{\partial \eta^2} + \bar{R}e\beta_5\left[F_\xi + \beta_1\beta_{2\xi}(f^2 - \frac{2}{\rho}) + 2\beta_2\left(F + \frac{\beta_1\rho_\xi}{\rho^2}\right) - \frac{\beta_1}{\rho}(\beta_{4\xi} - \eta\beta_{3\xi}) + \frac{\beta_1\rho_\xi}{\rho^2}(\beta_4 - \beta_3\eta)\right] \quad (17)$$

where $F = \frac{\beta_1}{2} f_\xi^2 = \beta_1 f f_\xi$. The subscript ξ in Eq. (17) denotes partial derivative with respect to ξ.

A higher order term F_ξ appears in Eq. (17). The system, therefore, can never be closed unless this higher order term is eliminated. In this study, we will truncate the higher order term F_ξ. But in addition to this

truncation, we will also modify some of the parameters which appear in Eq. (17). To determine which of the parameters are to be modified and how to modify them, we have to understand the source of the nonsimilarity of the present shock layer flow. For constant wall conditions (including constant wall temperature and constant surface mass injection), there are two sources of nonsimilarity. One is the pressure gradient imposed by the shock which is directly proportional to $\frac{d\ln u_s}{d\xi}$ and is represented by the parameter β_2; the other is the pressure gradient induced by the centrifugal force as represented by the parameters β_3 and β_4. The centrifugal pressure gradient will be important only in a thin layer near the surface (Ref. 8). Hence, the primary reason for the flow outside the entropy layer to be nonsimilar is due to the pressure gradient imposed by shock. In other words, outside the entropy layer, F_ξ is nonzero, primarily due to the fact that $\frac{d^2(\ln u_s)}{d\xi^2}$ is nonzero. Therefore, in order to be consistent with the truncation of F_ξ, the term proportional to $\frac{d^2\ln u_s}{d\xi^2}$ in the expression for $\beta_1\beta_{2\xi}$ must also be truncated. Based on this argument, it is then clear that the parameter $\beta_1\beta_{2\xi}$ which appears in Eq. (17) is to be modified. We will replace $\beta_1\beta_{2\xi}$ in Eq. (17) by β_6, and define β_6 as

$$\beta_6 = \beta_{1\xi}\beta_2 - 1 \tag{18}$$

We note that from the definitions of β_1, β_2 (Eq. (15)) and $\beta_{2\xi}$, that we find $\beta_{1\xi}\beta_2 \equiv \beta_1\beta_{2\xi} - \frac{d^2\ln u_s}{d\xi^2}$. Hence, β_6 is simply equal to $\beta_1\beta_{2\xi}$ minus the higher order ξ-derivative term plus a constant. The constant one in Eq. (18) is introduced in the expression for β_6 to ensure that β_6 is equal to $\beta_1\beta_{2\xi}$ at stagnation point (which is zero). We note at stagnation point $\beta_{1\xi} = 1$ and $\beta_2 = 1$.

After some numerical experiments, we found that in order to obtain the correct entropy layer behavior in the inviscid nonradiating case, it is also necessary to modify the parameter β_2 in Eq. (17). We replace β_2 in Eq. (17) with β_7, and define β_7 as:

$$\beta_7 = \frac{\beta_1^2}{u_s \beta_{1\xi}} \left[\frac{1}{u_s} \left(\frac{du_s}{d\xi} \right)^2 - \frac{d^2 u_s}{d\xi^2} \right] \tag{19}$$

The expression for β_7 is obtained from the relation that $\beta_{2\xi} = 0$ for all ξ. This can be demonstrated as follows: from Eq. (15) we have

$$\beta_{2\xi} = \frac{\beta_{1\xi}}{\beta_1} \beta_2 - \frac{\beta_1}{u_s^2} \left(\frac{du_s}{d\xi} \right)^2 + \frac{\beta_1}{u_s} \frac{d^2 u_s}{d\xi^2}$$

If $\beta_{2\xi} = 0$ for all ξ, it then implies $\beta_2 =$ Eq. (19). The physical reason for the successful application of the Eq. (19) is, however, not clear.

Based on above considerations, we therefore propose the following model equation for F :

$$f \frac{\partial^2 F}{\partial \eta^2} + 2 \bar{R}e \beta_5 \eta \frac{\partial F}{\partial \eta} + \left(\frac{F}{2f} - \frac{\beta_{5\xi} \beta_1}{2\beta_5} f \right) \frac{\partial^2 f}{\partial \eta^2}$$

$$= \bar{R}e \beta_5 \left[(\beta_{1\xi} \beta_2 - 1)(f^2 - \frac{2}{\rho}) + \frac{2\beta_1^2}{u_s} \left[\frac{1}{u_s} \left(\frac{du_s}{d\xi} \right)^2 - \frac{d^2 u_s}{d\xi^2} \right] \left(F + \frac{\beta_1 \rho_\xi}{\rho^2} \right) \right.$$

$$\left. - \frac{\beta_1}{\rho} (\beta_{4\xi} - \eta \beta_{3\xi}) + \frac{\beta_1 \rho_\xi}{\rho} (\beta_4 - \eta \beta_3) \right] \tag{20}$$

The model equation we have proposed here (Eq. (20)) is essentially a local similar equation for F under an effective pressure gradient which is different from the pressure gradient imposed by the shock. The validity of this equation cannot be argued rigorously. It can only be established by comparison with existing correct solutions. Therefore, it is the major purpose of this report to demonstrate the model equation (20).

We will now consider the energy equation. Again we obtain an equation for $\beta_1 H_\xi$ by differentiating Eq. (16) with respect to ξ and multiplying the resulting equation by β_1. We obtain

$$\frac{\partial}{\partial\eta}\left(\frac{F}{f}\frac{\partial H}{\partial\eta} + f\frac{\partial \bar{H}_\xi}{\partial\eta}\right) + \beta_1\left(2u_s\frac{du_s}{d\xi} - \frac{\beta_{5\xi}}{\beta_5}\right)(\text{Pr-1})\frac{\partial}{\partial\eta}\left(f^2\frac{\partial f}{\partial\eta}\right) - \frac{\beta_{5\xi}}{\beta_5}\frac{\partial}{\partial\eta}\left(f\frac{\partial H}{\partial\eta}\right)$$

$$+ u_s^2(\text{Pr-1})\frac{\partial^2}{\partial\eta^2}(fF) + \bar{R}e\beta_5 Pr\left[2\eta\frac{\partial \bar{H}_\xi}{\partial\eta} - \beta_1\bar{H}_{\xi\xi}\right.$$

$$\left. - \beta_1\left(\frac{\beta_1}{\epsilon\rho_s\mu_s r_s}\right)_\xi\sum_i\frac{\Gamma_i}{\lambda_i}\frac{\partial q_i}{\partial\eta} - \frac{\beta_1}{\epsilon\rho_s\mu_s r_s}\sum_i\frac{\Gamma_i}{\lambda_i}\frac{\partial q_{i\xi}}{\partial\eta}\right] = 0 \qquad (21)$$

where $\bar{H}_\xi = \beta_1 H_\xi$, $\bar{H}_{\xi\xi} = (\beta_1 H_\xi)_\xi$.

And again a higher order term $\beta_1\bar{H}_{\xi\xi}$ appears in Eq. (21). We now claim that, unlike the higher order term in the momentum Eq. (14), the term $\bar{H}_{\xi\xi}$ can be simply truncated. This is so because of the following argument. For constant wall temperature and quasi-one-dimensional radiative transport, there is no external source of nonsimilarity for temperature field. The nonsimilarity in temperature field is primarily due to nonsimilarity in velocity field. Therefore, to be consistent with the velocity field, for which we have derived a locally similar equation for F, we will assume $\bar{H}_\xi$ to be locally similar and assume in Eq. (21) that

$$\bar{H}_{\xi\xi} \equiv 0, \quad F \equiv 0 \qquad (22)$$

The equation for the term $\frac{\partial q_{i\xi}}{\partial\eta}$ in Eq. (21) is obtained simply by differentiating Eq. (9) and (10) with respect to ξ. This equation is

$$\frac{\partial q_{i\xi}}{\partial\eta} = -\lambda_i\left(\frac{r_s\alpha_i}{u}\right)_\xi[I_i - 4\pi B_i] - \frac{\lambda_i r_s\alpha_i}{u}[I_{i\xi} - 4\pi B_{i\xi}] \qquad (23)$$

with

$$\frac{\partial I_{i\xi}}{\partial \eta} = - 3\lambda_i \left[\left(\frac{r_s \alpha_i}{u} \right)_\xi q_i + \frac{r_s \alpha_i}{u} q_{i\xi} \right] \tag{24}$$

We have now completed our derivation of the model equations for the nonsimilar terms. They are Eqs. (20) to (24). The boundary conditions are:

At shock:

$$F = \bar{H}_\xi = 0 \ , \ I_{i\xi} - 2q_{i\xi} = 0 \quad \text{for all } i$$

At wall:

$$F = 0 \text{ (no slip)}, \ \bar{H}_\xi = 0 \text{ (constant wall temperature)}$$

and $I_{i\xi} + 2q_{i\xi} = 0$ for all i

This set of equations is to be coupled with Eqs. (9), (10), (11), (12), (14) and (16). We note that this is a set of ordinary differentiating equations. Solutions are to be sought locally. All the parameters appearing in the equations are functions of local shock conditions. We also note that in the calculation of $B_{i\xi}$ and $\alpha_{i\xi}$, we will need the expression of T_ξ. This again can be obtained by differentiating Eq. (12) with respect to ξ.

Section 3
METHOD OF SOLUTION

3.1 FORMAL SOLUTION FOR RADIATION FIELD

Let us define optical depth τ_i as

$$\tau_i = \lambda_i r_s \int_0^{\alpha_i} \frac{\alpha_i}{u}\, d\eta$$

It can be shown that the solutions to Eqs. (9), (10), (23) and (24) are given in terms of τ_i as

$$q_i = D_{i,1}\, e^{\sqrt{3}\,\tau_i} + D_{i,2}\, e^{-\sqrt{3}\,\tau_i} + \tfrac{1}{2}\,(\ell_{i,1}+\ell_{i,2})$$

$$I_i = \sqrt{3}\left[D_{i,2}\, e^{-\sqrt{3}\,\tau_i} - D_{i,1}\, e^{\sqrt{3}\,\tau_i} - \tfrac{1}{2}\,(\ell_{i,1}-\ell_{i,2})\right]$$

$$\frac{\partial q_i}{\partial \eta} = \frac{\lambda_i \alpha_i r_s}{u}\,[2S_i - I_i] \qquad (25)$$

$$\frac{\partial q_{i\xi}}{\partial \eta} = \frac{\lambda_i \alpha_i r_s}{u}\sqrt{3}\left\{C_{i,1}\, e^{\sqrt{3}\,\tau_i} - C_{i,2}\, e^{-\sqrt{3}\,\tau_i} + \tfrac{1}{2}\left[\mathcal{L}_{i,1} - \mathcal{L}_{i,2} + \frac{2}{\sqrt{3}}\, Q_i\right]\right\} \qquad (26)$$

with $$\mathcal{L}_{i,1} = e^{\sqrt{3}\,\tau_i} \int_0^{\tau_i} e^{-\sqrt{3}\,\tau_i} \left[Q_i + \sqrt{3}\left(\ln \frac{r_s \alpha_i}{u}\right)_\xi q_i\right] d\tau_i$$

$$\mathcal{L}_{i,2} = e^{-\sqrt{3}\,\tau_i} \int_0^{\tau_i} e^{\sqrt{3}\,\tau_i} \left[Q_i - \sqrt{3}\left(\ln \frac{r_s \alpha_i}{u}\right)_\xi q_i\right] d\tau_i$$

$$\ell_{i,1} = e^{\sqrt{3}\,\tau_i} \int_0^{\tau_i} S_i\, e^{-\sqrt{3}\,\tau_i}\, d\tau_i$$

$$\mathcal{L}_{i,2} = e^{-\sqrt{3}\,\tau_i} \int_0 S_i e^{\sqrt{3}\,\tau_i}\, d\tau_i$$

$$S_1 = 4\pi \frac{B_i}{\alpha_1} \quad , \quad S_2 = 4\pi B_2 \quad , \quad S_3 = 4\pi B_3$$

$$Q_i = \left(\ln \frac{r_s B_i}{u}\right)_\xi S_i - \left(\ln \frac{r_s \alpha_i}{u}\right)_\xi I_i \qquad i = 1,2,3$$

and $$C_{i,1} = -\frac{2+\sqrt{3}}{2-\sqrt{3}} C_{i,2} \qquad D_{i,1} = -\frac{2+\sqrt{3}}{2-\sqrt{3}} D_{i,2}$$

$$C_{i,2} = \frac{\mathcal{L}_{i,1}(\tfrac{1}{2}) + (2-\sqrt{3})^2\, \mathcal{L}_{i,2}(\tfrac{1}{2})}{2\left[(2+\sqrt{3})^2 e^{\sqrt{3}\,\tau_i(\frac{1}{2})} - (2-\sqrt{3})^2 e^{-\sqrt{3}\,\tau_i(\frac{1}{2})}\right]}$$

$$D_{i,2} = \frac{\mathcal{L}_{i,1}(\tfrac{1}{2}) + (2-\sqrt{3})^2\, \mathcal{L}_{i,2}(\tfrac{1}{2})}{2\left[(2+\sqrt{3})^2 e^{\sqrt{3}\,\tau_i(\frac{1}{2})} - (2-\sqrt{3})^2 e^{-\sqrt{3}\,\tau_i(\frac{1}{2})}\right]}$$

For a given temperature and pressure field, the radiation field is therefore given by a straightforward integration.

3.2 INVISCID CASE

When $\bar{R}e \to \infty$, no stretching of the x coordinate is necessary. Therefore, $\xi = x$ and the momentum and energy equations become

$$\frac{\partial u_2}{\partial \eta} = \frac{F + \beta_2(u_2 - \frac{2}{\rho}) - \frac{1}{\rho}(\beta_4 - \beta_3\eta)}{\eta} \tag{27}$$

$$\frac{\partial F}{\partial \eta} = \frac{\beta_6(u_2 - \frac{2}{\rho}) + 2\beta_7(F + \frac{\beta_1\rho_\xi}{\rho^2}) - \frac{\beta_1}{\rho}(\beta_{4\xi} - \eta\beta_{\xi\xi}) + \frac{\beta_1\rho_\xi}{\rho^2}(\beta_4 - \beta_3\eta)}{2\eta} \tag{28}$$

$$\frac{\partial H}{\partial \eta} = \frac{1}{2\eta}\left(\bar{H}_\xi + \frac{\beta_1}{r_s}\sum_i \frac{\Gamma_i}{\lambda_i}\frac{\partial q_i}{\partial \eta}\right) \tag{29}$$

$$\frac{\partial \bar{H}_\xi}{\partial \eta} = \frac{\beta_1}{2\eta}\left[\left(\frac{\beta_1}{r_s}\right)_\xi \sum_i \frac{\Gamma_i}{\lambda_i}\frac{\partial q_i}{\partial \eta} + \frac{\beta_1}{r_s}\sum_i \frac{\Gamma_i}{\lambda_i}\frac{\partial q_{i\xi}}{\partial \eta}\right] \tag{30}$$

where $u_2 = f^2$ and $u_{2\xi} = f_\xi^2$. In seeking the solution, we first assume a profile of H and H_ξ , then from Eqs. (27) and (28), we obtain u_2 and $u_{2\xi}$ and from Eqs. (25) and (26), we obtain the profiles of $\frac{\partial q_i}{\partial \eta}$ and $\frac{\partial q_{i\xi}}{\partial \eta}$. Using these profiles, we can obtain new profiles for H and H_ξ from Eqs. (29) and (30). We keep iterating on H and H_ξ until they converge. In the integration of Eqs. (27) to (30), however, singularities exist at the wall due to the fact that $\eta = 0$ at the wall. This is an integrable singularity and is a node point. In the actual computation in order to avoid numerical difficulties, we carried the integration to $\eta = 10^{-4}$ instead of to $\eta = 0$. The effect of this approximation on the radiative flux to the wall is negligibly small. The boundary conditions at wall are abandoned for inviscid cases.

3.3 VISCOUS CASE WITHOUT SURFACE MASS INJECTION

For a viscous case, it is found to be convenient to introduce another independent variable ω, defined as

$$\frac{d\eta}{d\omega} = \omega_s f \qquad \omega_s = \frac{0.5-\eta_\omega}{\int_0^1 f d\omega} \tag{31}$$

hence the range of ω will be from zero to one.

In terms of ω, a formal solution can be obtained for f as

$$f = G_1(\omega) + C_f G_2(\omega) \tag{32}$$

with
$$G_1(\omega) = \bar{R}e\omega_s^2\beta_5 \int_0^\omega d\omega' \int_0^{\omega'} e^{2\bar{R}e\omega_s\beta_5\int_{\omega'}^{\omega''}\eta d\omega''} \left[F + \beta_2(f^2-\frac{2}{\rho}) - \frac{\beta_4-\beta_3\eta}{\rho}\right] d\omega''$$

$$G_2(\omega) = \int_0^\omega e^{-2\bar{R}e\omega_s\beta_5\int_0^{\omega'}\eta d\omega''} d\omega' \tag{33}$$

where

$$F = ff_\xi\beta_1 \qquad C_f = \frac{1-G_1(1)}{G_2(1)}$$

Similarly, one can write down the formal solution for F and for the energy equation H and H_ξ as follows:

$$F = G_3(\omega) + C_f G_4(\omega) \tag{34}$$

with
$$G_3 = \int_0^\omega f d\omega' \int_0^{\omega'} e^{2\bar{R}e\omega_s\beta_s\int_{\omega'}^{\omega''}\eta d\omega'} g_F d\omega''$$

$$g_F = \left(\frac{\beta_1\beta_{5\xi}}{\beta_5} - \frac{F}{f^2}\right)\frac{\partial^2 f}{\partial\omega^2} + \bar{R}e\beta_5\omega_s^2\left[F\beta_{1\xi} + \beta_1\beta_{2\xi}(f^2-\frac{2}{\rho})\right.$$

$$\left. + \beta_2\left(2F + \frac{2\beta_1\rho_\xi}{\rho^2}\right) + \frac{\beta_1\rho_\xi(\beta_4-\beta_3\eta)}{\rho^2} - \frac{\beta_1(\beta_{4\xi}-\beta_{3\xi}\eta)}{\rho}\right] \tag{35}$$

$$G_4 = \int_0^{\omega} f\, e^{-2\bar{R}e\beta_5\omega_s \int_0^{\omega'} \eta d\omega''} d\omega'$$

$$C_F = \frac{-G_3(1)}{G_4(1)}$$

$$H = G_5(\omega) + C_H G_6(\omega) + H_w - \frac{u_s^2}{2}(Pr-1) f^2$$

with

$$G_5(\omega) = \bar{R}ePr\omega_s^2\beta_5 \int_0^{\omega} d\omega' \int_0^{\omega} e^{2\bar{R}e\omega_s\beta_5 Pr \int_{\omega'}^{\omega''} \eta d\omega''} \left[f\bar{H}_\xi + \frac{\beta_1}{\epsilon\rho_s\mu_s u_s} \sum_i \Gamma_i \alpha_i \frac{\partial q_i}{\partial \tau_i} + u_s^2(Pr-1)\eta \frac{\partial f^2}{\partial \omega} \right] d\omega''$$

$$G_6(\omega) = \int_0^{\omega} e^{-2\bar{R}ePr\omega_s\beta_5 \int_0^{\omega'} \eta d\omega''} d\omega'$$

$$C_H = \frac{1 - G_5(1) - H_w + \frac{u_s^2}{2}(\beta_2 - 1)}{G_6(1)} \qquad (37)$$

where H_w is the total enthalpy at wall, $\bar{H}_\xi = \beta_1 H_\xi$ and the equation for $\bar{H}_\xi$ is

$$\bar{H}_\xi = G_7(\omega) + G_8(\omega) + C_{\bar{H}_\xi} G_9(\omega) + \bar{H}_{\xi w} \qquad (38)$$

with

$$G_7(\omega) = \bar{R}ePr\beta_5\omega_s \int_0^{\omega} d\omega' \int_0^{\omega'} e^{2\bar{R}ePr\omega_s\beta_5 \int_{\omega'}^{\omega''} \eta d\omega''} g_{\bar{H}_\xi} d\omega''$$

$$g_{\bar{H}_\xi} = 2\eta\left[u_s \frac{du_s}{d\xi}(Pr-1)\beta_1 \frac{\partial f^2}{\partial \omega}\right]$$

$$- \omega_s \beta_1 \left[\frac{\beta_1}{\epsilon \rho_s \mu_s u_s} + \frac{r_s}{u_s}\left(\frac{\beta_1}{\epsilon \rho_s \mu_s r_s}\right)_\xi\right] \sum_i \Gamma_i \alpha_i \frac{\partial q_i}{\partial \tau_i} + \frac{\beta_1^2 \omega_s}{\epsilon \rho_s \mu_s u_s} \sum_i \Gamma_i \alpha_i \frac{\partial q_{i\xi}}{\partial \tau_i}$$

$$- \frac{2\beta_1 \beta_{5\xi}}{\beta_5} \eta \frac{\partial H}{\partial \omega} + \omega_s f \bar{H}_\xi \left(\frac{\beta_1 \beta_{5\xi}}{\beta_5} + \beta_{1\xi}\right) \qquad (39)$$

$$G_8(\omega) = -\int_0^\omega \left[u_s \frac{du_s}{d\xi}(Pr-1)\beta_1 \frac{\partial f^2}{\partial \omega}\right] d\omega$$

$$G_9(\omega) = \int_0^\omega e^{-2\bar{R}e\beta_5 \omega_s \int_0^\omega \eta d\omega} d\omega$$

$$C_{\bar{H}_\xi} = \frac{-(G_7(1)+G_8(1)+\bar{H}_{\xi w})}{G_9(1)}$$

where $\bar{H}_{\xi w} = \beta_1 \frac{\partial H}{\partial \xi}$ at wall.

In seeking the solution to Eqs. (31) to (38), we first guess the profiles (as function of ω) of f, F, H and $\bar{H}_\xi$. Using these guessed profiles, one can calculate the radiation field, and the new profiles from Eqs. (31) through (38). One, therefore, has to iterate on these profiles until they converge to a solution.

3.4 VISCOUS CASE WITH CONSTANT SURFACE MASS INJECTION

In cases of surface mass injection, one notes that $\eta_w = \frac{\rho_w v_w}{\rho_\infty u_\infty}$ is negative. Hence, the term $e^{-2\bar{R}ePr\omega_s\beta_5\int_0^\omega \eta d\omega}$ may become exponentially large. If this happens, we will have numerical accuracy

problems and solutions become extremely difficult to obtain. Physically, if the injection rate is too large, such that the boundary layer is effectively blowing off the wall, we will essentially have a shock layer which consists of an inviscid inner layer near the wall, an inviscid outer layer near the shock, and a viscous layer in between. If one integrates the equation from wall to shock or vice versa, it is then equivalent to seek a solution for boundary layer flow by integrating the equation from the inviscid region to the wall. This is not only ineffective, but also numerically impossible.

In order to avoid these difficulties, we have derived the following scheme for the case of large injection rates: First, we guess a profile for f. From this guessed profile, we find ω_o such that $\eta(\omega_o) = 0$, then we choose ω_o as our starting point and integrate the equation from ω_o to 0 and from ω_o to one separately. The starting value is determined by the condition that the slope must be continuous at ω_o. To be more specific, let us consider the momentum equation (equation for f). Let us denote f^+ be the solution for f from ω_o to one, and f^- be the solution for f from $\omega_o \to 0$. Then, from Eq. (32), we can write

$$f^+ = G_1^+ + C_f^+ G_2^+ + f(\omega_o)$$

$$f^- = G_1^- + C_f^- G_2^- + f(\omega_o)$$

where the function G^+ is integrated from ω_o to 1 and G^- is integrated from ω_o to 0. From the boundary condition $f^-(o) = 0$ and $f^+(1) = 1$, we have

$$C_f^+ = \frac{(1-G_1^+(1)-f(\omega_o))}{G_2^+(1)} \qquad \text{and} \qquad C_f^- = \frac{-(G_1^-(o)+f(\omega_o))}{G_2^-(o)} \quad .$$

So far $f(\omega_o)$ is still unknown. In order to determine $f(\omega_o)$, we invoke the condition that the slope of f at ω_o must be continuous. Hence, we have $\frac{\partial f^+}{\partial \omega} = \frac{\partial f^-}{\partial \omega}$ at ω_o. From this relation, one can find an expression for $f(\omega_o)$ in terms of G's and their derivative. Similarly, one can obtain solutions for F, h and $\bar{H}_\xi$.

Section 4

RESULTS

4.1 COMPARISONS WITH EXISTING SOLUTIONS

In order to establish the validity of the solution based on the present locally nonsimilar method, we will compare our present solutions with existing numerical ones. Figure 2 shows the total enthalpy profiles for viscous cases at stagnation point. Comparison is made with a detailed numerical calculation. One can see that the agreement is excellent in both the enthalpy profile and radiative flux to the wall. The same comparison was made before in Ref. 1. In that comparison, we found the agreement was relatively poor. It has been determined that the reason for that relatively poor agreement was due to a discrepancy in the calculation of the degree of ionization. The degree of ionization φ is given by the following equation:

$$\frac{\varphi^2}{1-\varphi^2} = a\left(\frac{2\pi m_e}{h^2}\right)^{3/2} \frac{(kT)^{5/2}}{P} e^{-\theta_i/T} \tag{39}$$

The constant a is equal to 2 in Ref. 1, while in Ref. 9 the constant is equal to 4.5. The value 4.5 is found to be the right one since it is based on the correct statistical weight for the nitrogen ion. In this paper, the constant is taken to be 4.5 throughout, except when we make comparisons with the solution given by Ref. 1.

Figure 3 shows the comparison with Olstad's numerical solution (Ref. 2) for the nonradiating inviscid case for a 45° blunted cone at u_∞ = 12.2 km/sec and $\rho_\infty = 2.88 \times 10^{-7}$ gr/cm^3. It is seen that both the static enthalpy and the velocity profile given by the present solution are in good agreement with numerical

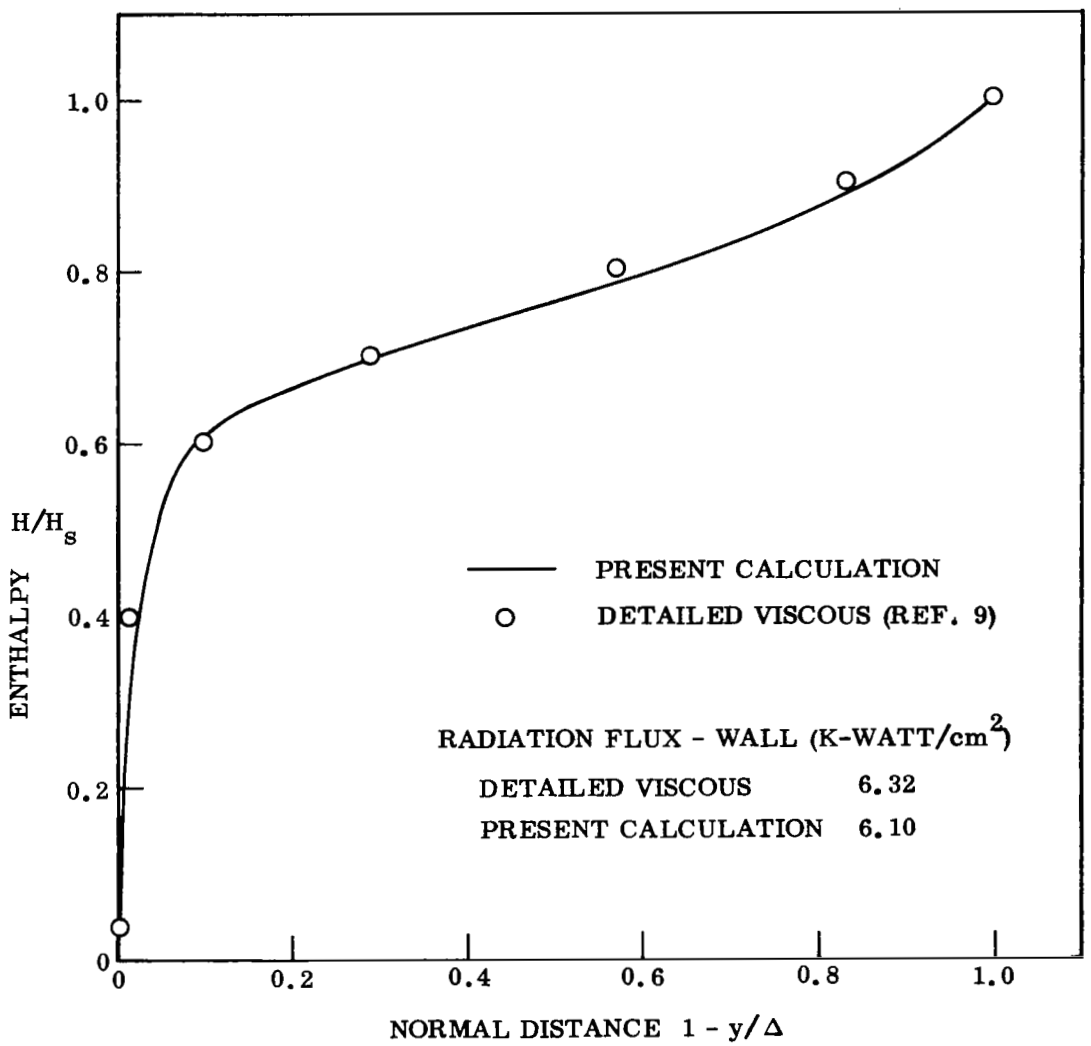

Fig. 2 Viscous Static Enthalpy Profile at Stagnation Point
V_∞ = 16 km/sec, $\rho_\infty = 4.21 \times 10^{-7}$ gm/cm^3, R_s = 234 cm

ones through the shock layer, except at the wall. The reason for the large discrepancy of the wall value is due to the fact that in the present solution, the integration of the equation did not carry all the way to the wall because of numerical difficulties (for detailed discussion see method of solution section). The present method gives a somewhat lower velocity profile as r_s increases; but one can see from this figure that the present solution is everywhere within 10% of the numerical one for r_s up to 4. At this point, the shock angle is nearly at its asymptotic value, and one expects that the profiles will change very little from this point on.

Comparisons are also made with Olstad's solution* for a radiating inviscid case. In this case, the freestream conditions are given as $u_\infty = 1.6$ km/sec, $\rho_\infty = 4.425 \times 10^{-7}$ gr/cm^3 and the shock is assumed to be given by the following equation

$$z_s = \frac{r_s^2}{1+1.026\, r_s} \tag{40}$$

with shock nose radius of 0.5 m. To make our solution consistent with those of Olstad, we have used a perfect gas equation of state, $\frac{P}{P_s} = \rho/\rho_s(h/h_s)$, instead of the $\frac{P}{P_s} = \rho/\rho_s(h/h_s)^{0.84}$ relation employed elsewhere in our calculations. Care has been taken to ensure that the radiation transport models are essentially identical in these two calculations. Unfortunately, there is a slight difference in the computation of the total number density. In the present calculation, the total number density is assumed to be given by,

$$N_t = \frac{\rho}{M} \tag{41}$$

*The author is indebted to Dr. W. B. Olstad for providing the numerical solutions.

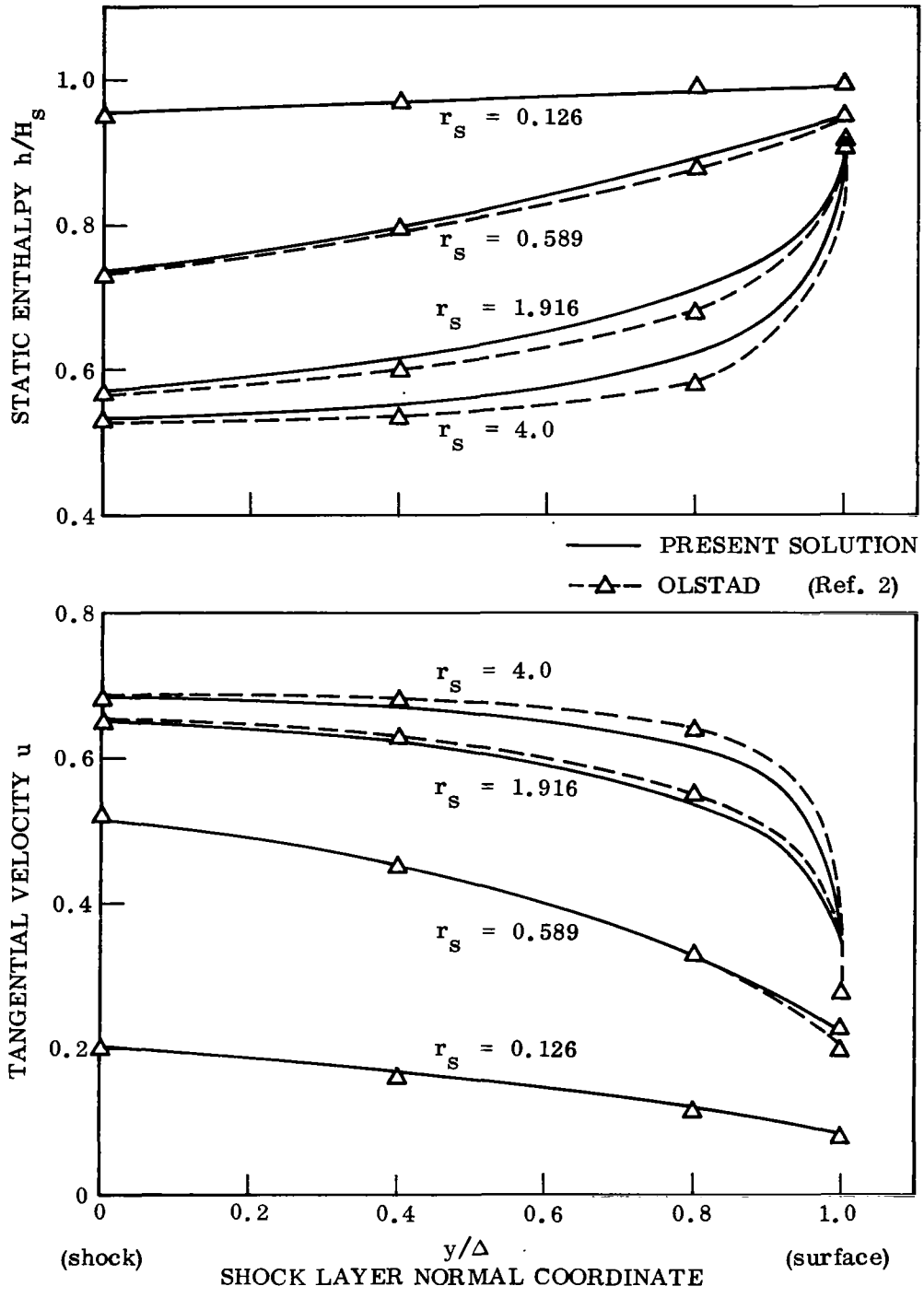

Fig. 3 Comparison of Present Locally Nonsimilar Blunt Cone Solution with Olstad's Streamline Marching Calculation (Adiabatic Case)

where M is the mass of a nitrogen atom, while in Olstad's calculation

$$N_t = \frac{P}{kT} \tag{42}$$

Eq. (41) will yield a number density somewhat lower than that of Eq. (42) in the stagnation region, but they are approximately equal far downstream from the stagnation region. Thus our present calculation will give a lower radiative flux to the wall than that given by Olstad's calculation in the stagnation region. The summary of the comparisons for this case are shown in Figs. 4 to 6. In Fig. 4, the given shock shape together with the calculated body shape are plotted. One can see that the body shape given by the present solution agrees very well with Olstad's solution. The static enthalpy profiles are compared in Fig. 5 for various r_s stations. Since the validity of Olstad's solution is not exactly known at the stagnation point, we thus start our comparison a small distance away from the stagnation point ($r_s = 0.134$). The profiles again are in very good agreement. Figure 6 shows the distribution of the radiative flux to the wall. They are all normalized by the value obtained from Olstad's solution at $r_s = 0.134$. The present solution shows a lower value at $r_s = 0.134$ than Olstad's value. Again this reflects the discrepancy in the computation of total number densities. At $r_s = 1.0$, the present solution shows a slightly higher value (by approximately 5%) than Olstad's value, and at $r_s = 3.0$, the present solution again shows lower value (by approximately 10%). This nonmonotonic behavior seems to be strange, but one has to realize that the radiative flux is a very sensitive function of static enthalpy. A small change in the enthalpy profile results in a large difference in radiative flux. In view of the approximate nature of the present solutions,

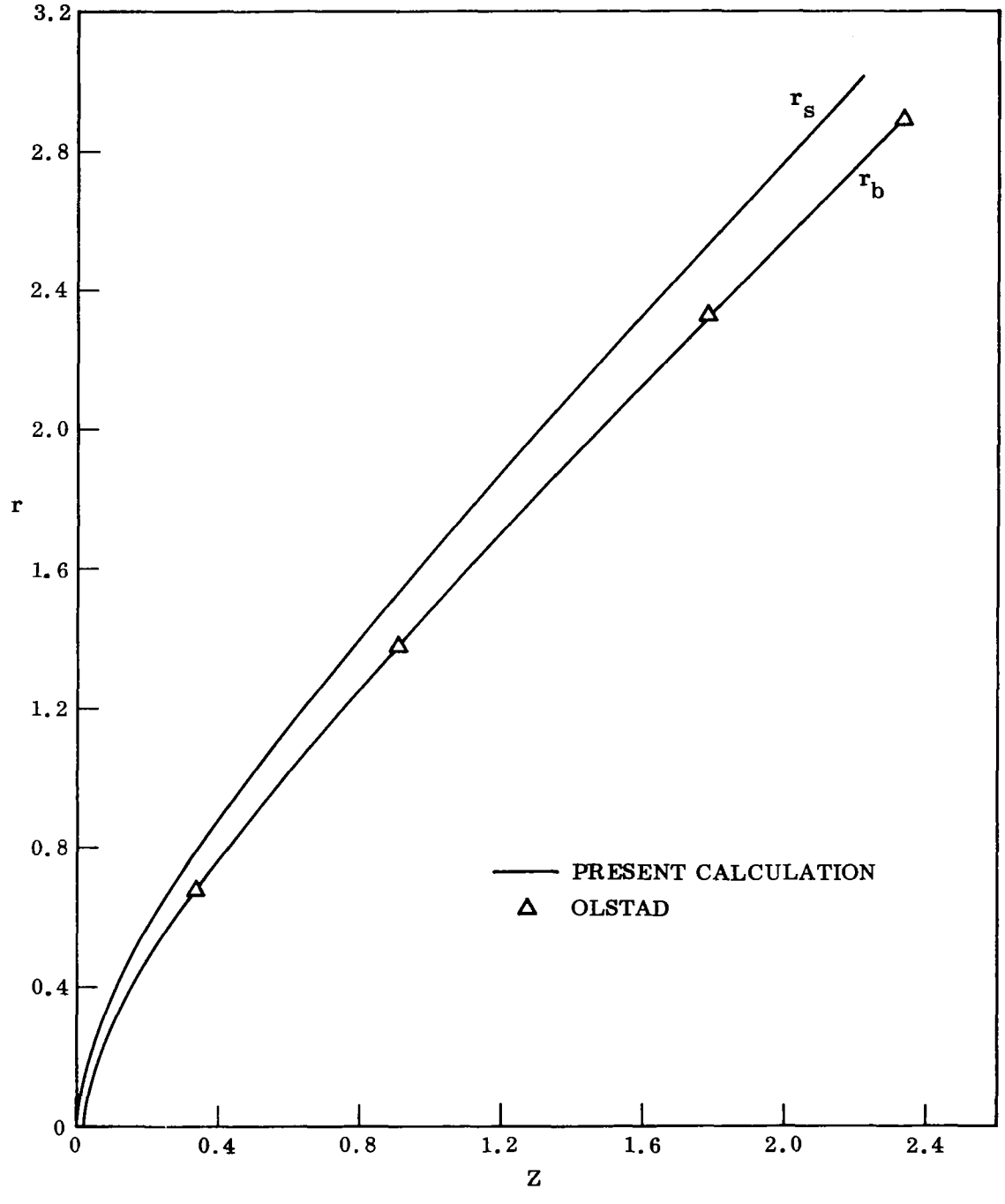

Fig. 4 Shock and Body Shapes, U_∞ = 16 km/sec, $\rho_\infty = 4.42 \times 10^{-7}$ gr/cm^3, R_s = 50 cm

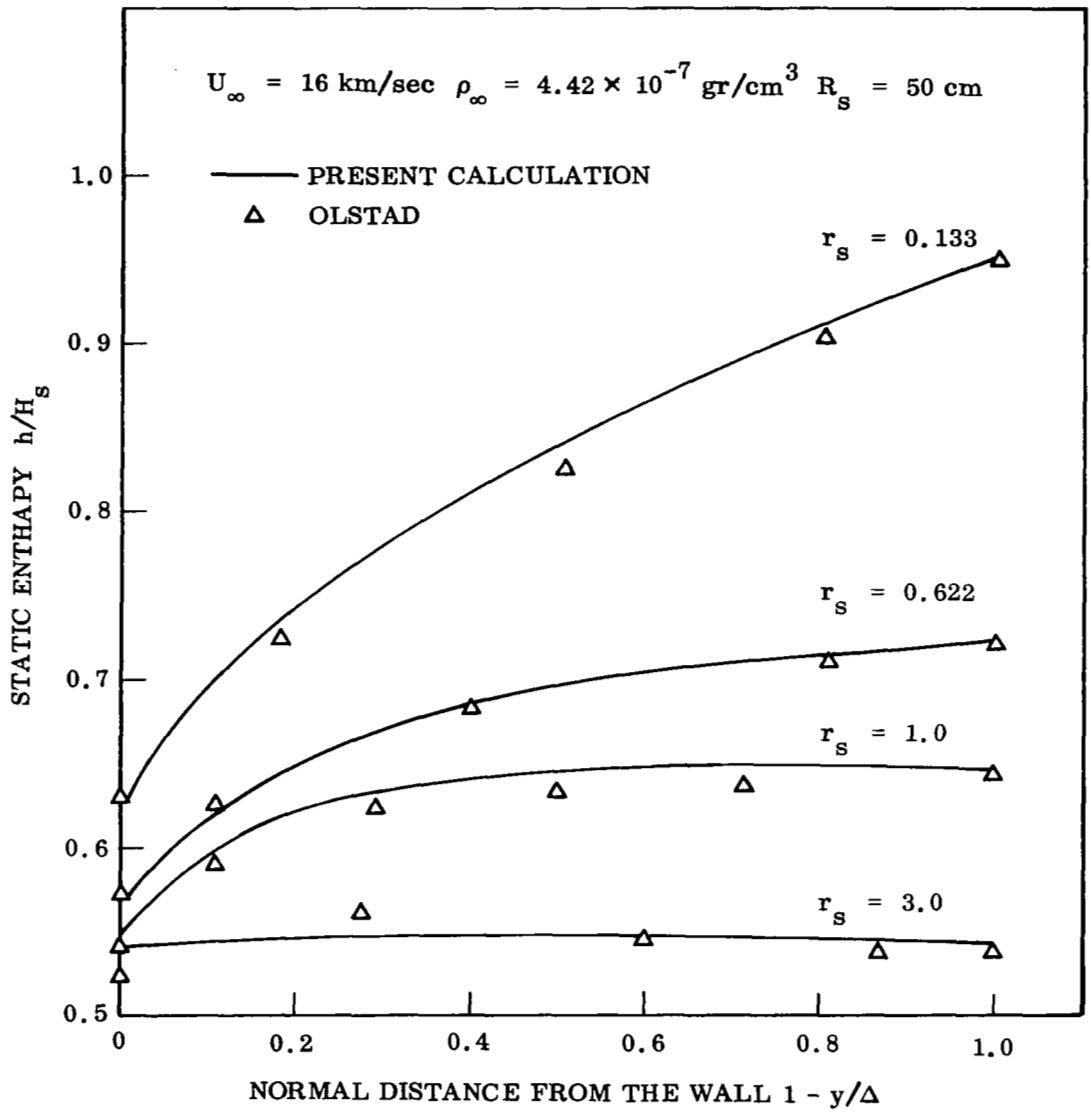

Fig. 5 Comparison of Present Locally Nonsimilar Blunt Cone Solution with Olstad's Streamline Marching Calculation (Radiating Flow Case)

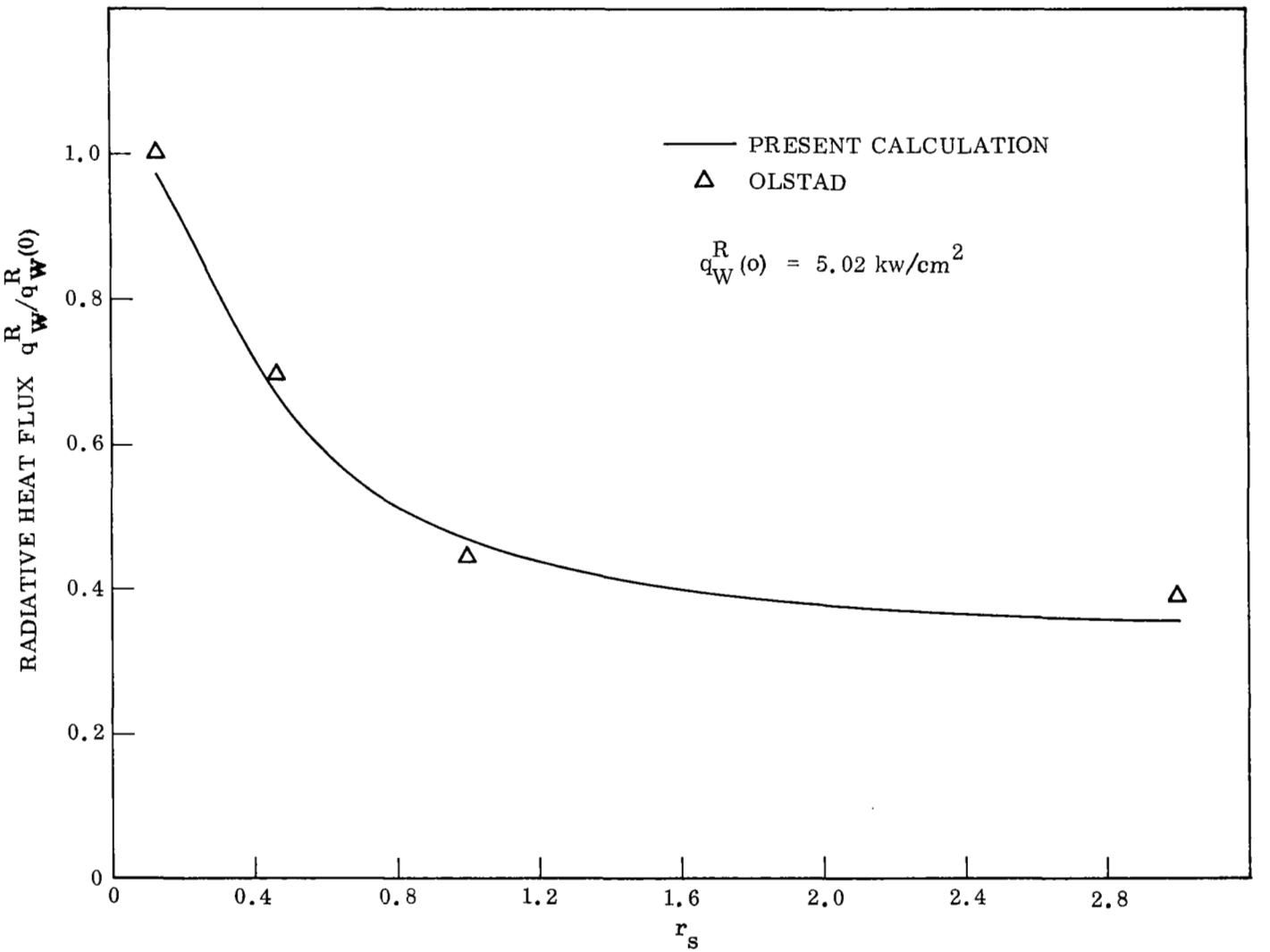

Fig. 6 Radiative Heat Flux Distribution for 45° Blunted Cone, U_∞ = 16 km/sec, $\rho_\infty = 4.42 \times 10^{-7}$ gr/cm^3, R_s = 50 cm

and some uncertainties involved in the Olstad's solutions, such as interpolations, iterations, etc., the discrepancies appearing in Fig. 6 seem to be entirely reasonable. From this comparison with the best currently available solution, we have established the validity of the present approximate method in treating inviscid radiating shock layers.

To establish the validity of present solutions for viscous cases (both radiating and nonradiating), similar comparisons should be made. Unfortunately, highly accurate, e.g., full numerical treatments, of viscous radiating shock layer flows far from stagnation region are simply not available. Indeed, even for the nonradiating case, solutions for high Reynolds number shock layer flow away from the stagnation region are unavailable. In order to present at least some qualitative idea of the applicability and validity of the present method for viscous cases, we will compare our present work with our previous series solution given in Ref. 1. The difficulties in comparing these solutions are that in Ref. 1, the series solution is given for a sphere and the coordinate system is body oriented. In the present formulation, the coordinate system is shock oriented. Therefore, even if the same shock shape is used in the present calculation, the calculated body shape may not be exactly a sphere. Despite this difficulty, we feel it is reasonable to make a comparison near the nose since the body obtained from our current solution will be nearly spherical, and the shock is nearly concentric with the body. The comparisons of radiative flux to the wall and the total enthalpy profile at $\theta = 30^\circ$ are given in Figs. 7 and 8. In the present calculation, the shock shape is taken exactly as that of in Ref. 1. The comparisons are based on the assumptions that the body is a sphere and the shock is concentric with a sphere in the region of interest. From Figs. 7 and 8,

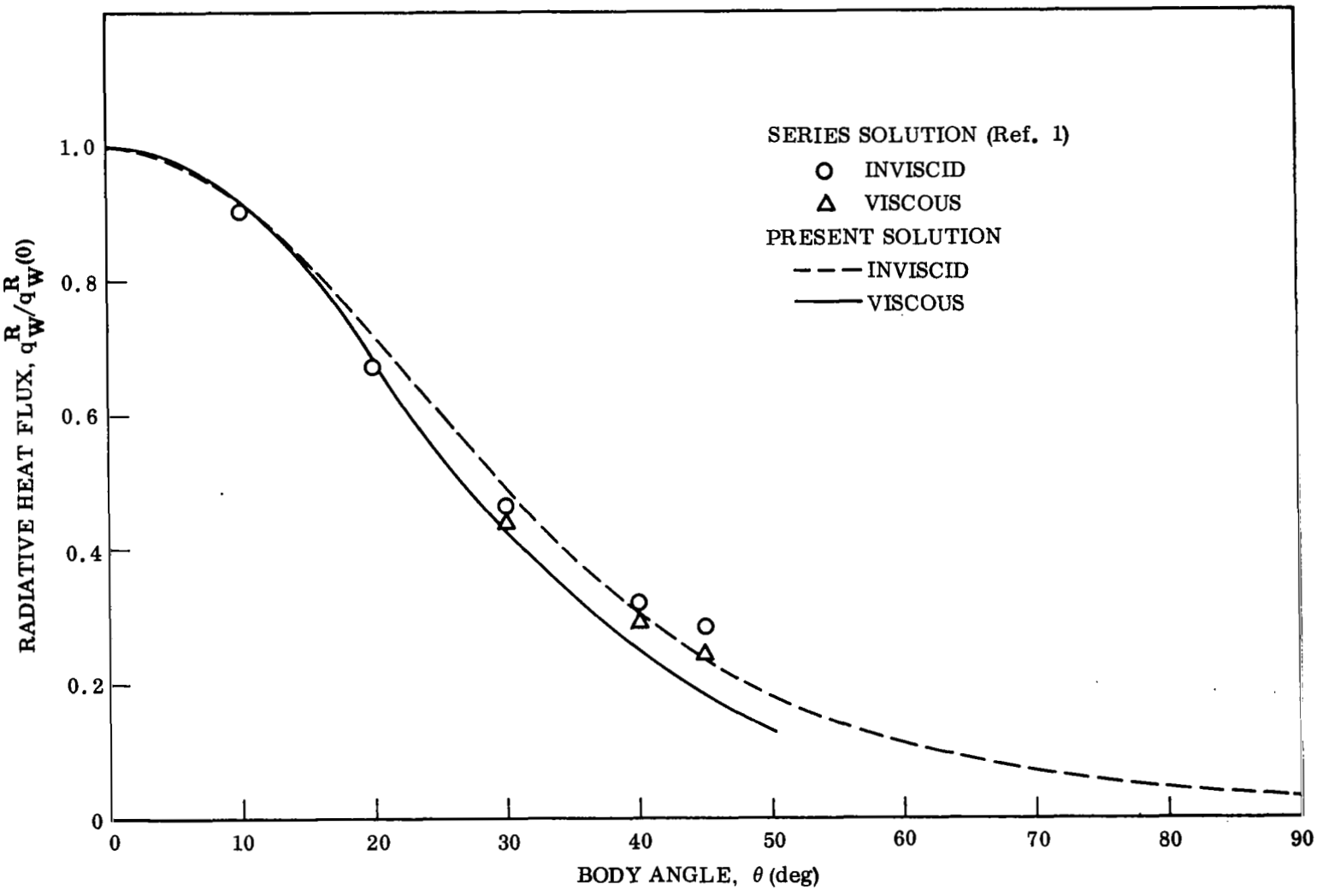

Fig. 7 Radiative Heat Flux Distribution for Sphere, U_∞ = 16 km/cm, $\rho_\infty = 4.21 \times 10^{-7}$ gr/cm^3, R_s = 234 cm

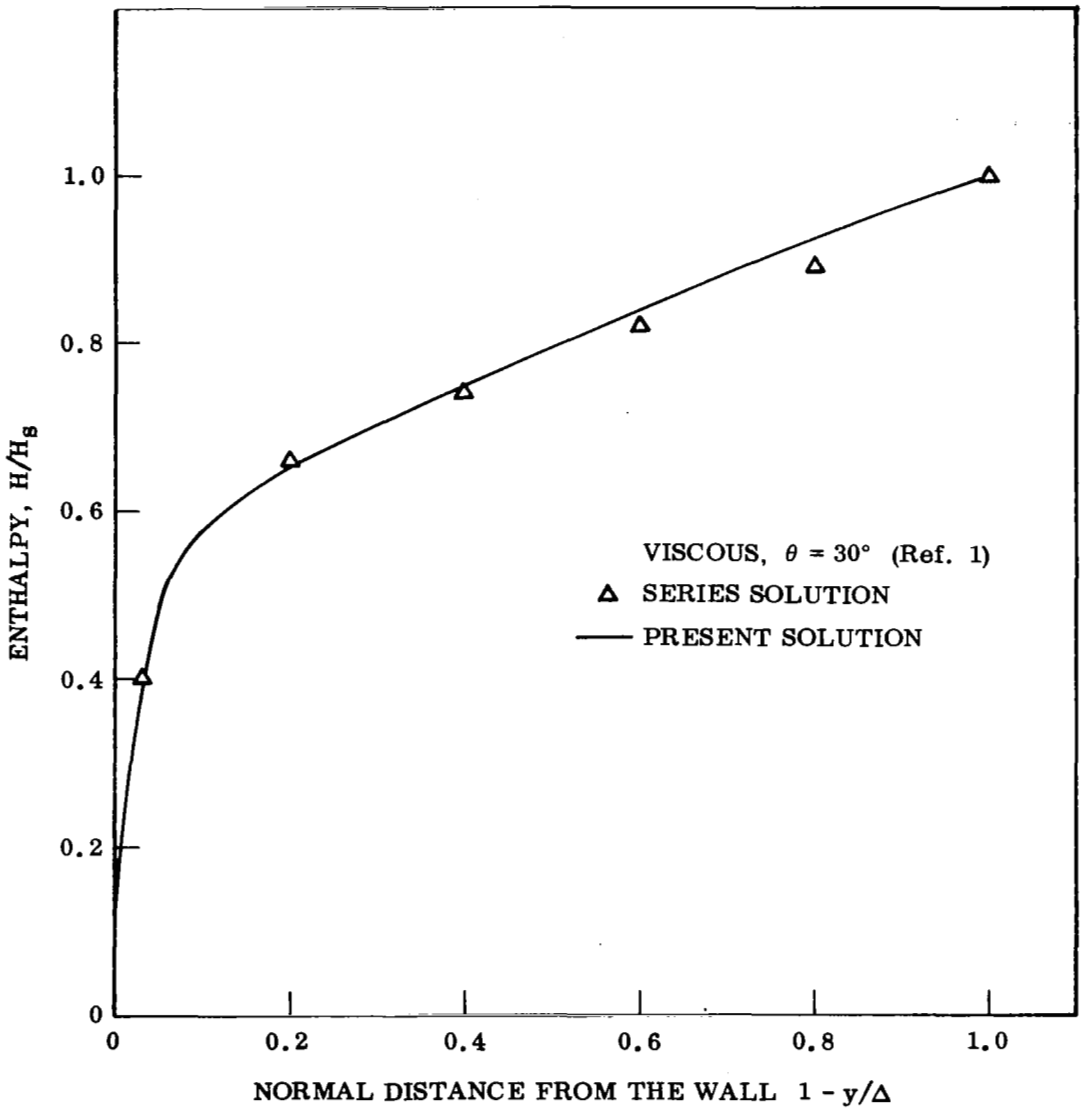

Fig. 8 Total Enthalpy Profile for Sphere at $\theta = 30°$, $U_\infty = 16$ km/cm, $\rho_\infty = 4.21 \times 10^{-7}$ gr/cm^3, $R_s = 234$ cm

one sees that the agreements are good for both the radiative heat flux distribution and the enthalpy profile. In Fig. 7, the comparison for the radiative heat flux distribution for an inviscid case is also presented.

4.2 TYPICAL SOLUTIONS

In the last section, we have made comparisons with existing solutions. Good agreement was found for all the cases and therefore we have reasonably established the validity of the present approach for thin shock layer problems. In this section we will present typical solutions for both the inviscid and the viscous cases and make some observations about these solutions. The data needed for the calculations are as follows:

Shock shape $z_s = \dfrac{r_s^2}{2+1.026\, r_s}$

Flight Conditions $u_\infty = 16$ km/sec, $\rho_\infty = 4.21 \times 10^{-7}$ gr/cm^3

$R_s = 234$ cm , $\varepsilon = 0.057$

Transport parameters $Pr = 0.72$, $\bar{R}e = 641$

Wall Condition $H_w = 0.0385$ (constant temperature) $\eta_w = 0$

The solutions are presented in Figs. 9 to 13. In Fig. 9, shock and body shape are plotted. From this figure one sees that radiation cooling does not change the body shape too much. Also, the viscous effect on the body shape is negligibly small. Figure 10 shows the static enthalpy profile across the shock layer for inviscid cases. Comparing the radiating profile with the nonradiating one, we see that for the present flight condition, substantial

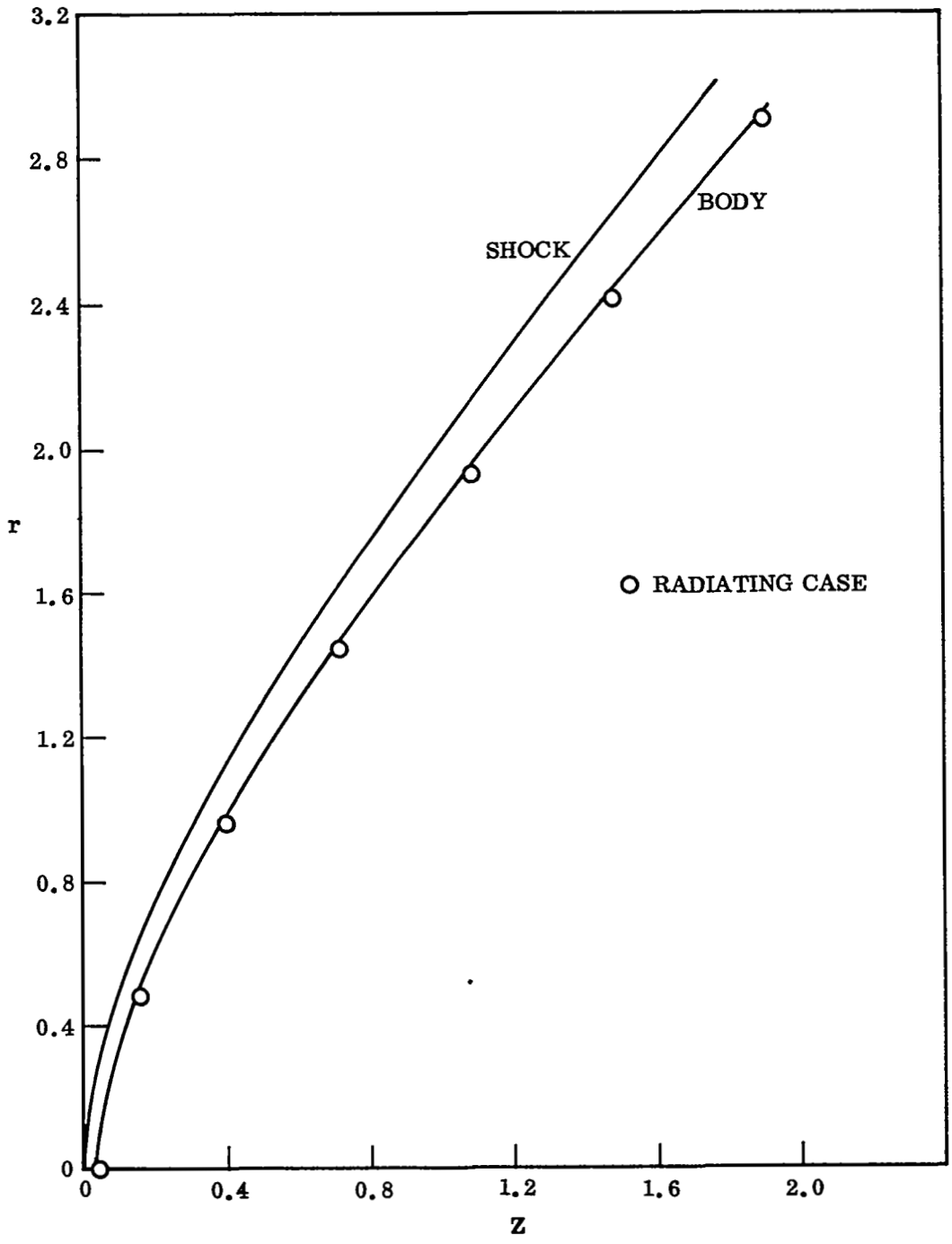

Fig. 9 Shock and Body Shapes, U_∞ = 16 km/cm, $\rho_\infty = 4.21 \times 10^{-7}$ gr/cm^3, R_s = 234 cm

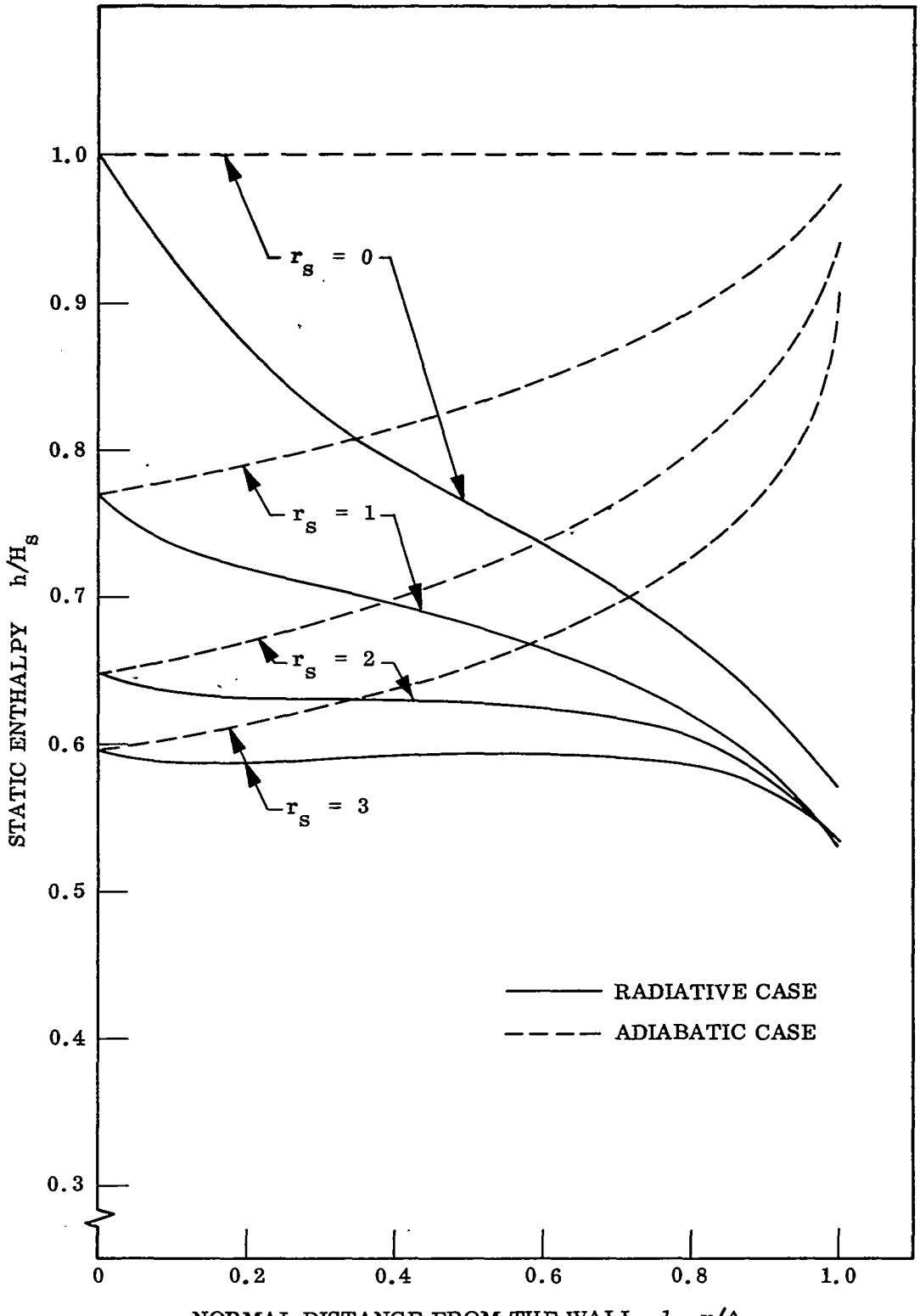

Fig. 10 Inviscid Static Enthalpy Profile
U_∞ = 16 km/cm, ρ_∞ = 4.21 x 10^{-7} gr/cm^3,
R_s = 234 cm

cooling is experienced through the shock layer. The nonradiating profiles show the growing of the entropy layer, while the radiating profiles show no entropy layer. The entropy layer, therefore, is being destroyed by radiative cooling. At far downstream, the radiating enthalpy profile indicates that the shock layer is nearly isothermal.

Figure 11 shows the static enthalpy profiles for viscous cases. The profiles are different from that of inviscid cases only in the region near the wall. This is because the wall is cold, and boundary layer effect brings down the gas temperature near the wall. The effect of this boundary layer on the radiative flux to the wall will be discussed later. The tangential velocity profiles are shown in Fig. 12. By comparing the profiles for radiating cases and that of nonradiating ones, we found the effect of radiative cooling on the velocity profiles is indeed small. This implies that the effect of radiative cooling is mostly thermodynamical, rather than dynamical. The same conclusion has been obtained in Ref. 1. The surface radiative flux distribution along the body is plotted in Fig. 13. The flux is normalized by the inviscid value at stagnation point. We find that the effect of viscosity at the stagnation point reduces the radiative flux by approximately 5%. Far away from the stagnation point, however, the viscous flux approaches the inviscid value. This is due to the relative thinning of the boundary layer far from the stagnation point. Hence the flow becomes dominated by the inviscid structure. For the conical body studied, the effect of the viscous flow on the radiative flux to the wall is small. A similar conclusion has been obtained previously for the flow past a sphere in Ref. 1.

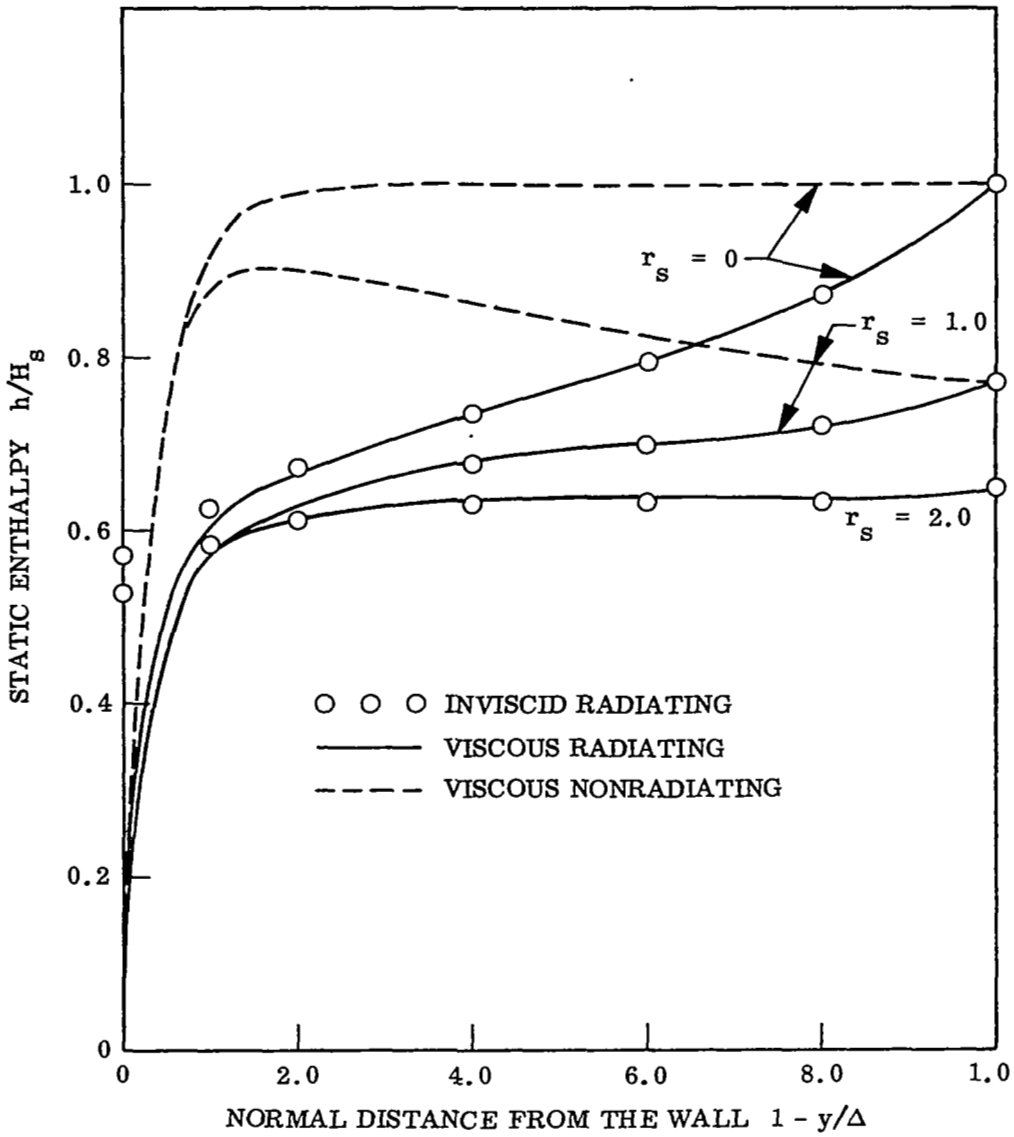

Fig. 11 Viscous Static Enthalpy Profile for a Blunted Cone
U_∞ = 16 km/cm, $\rho_\infty = 4.21 \times 10^{-7}$ gr/cm^3, R_s = 234 cm

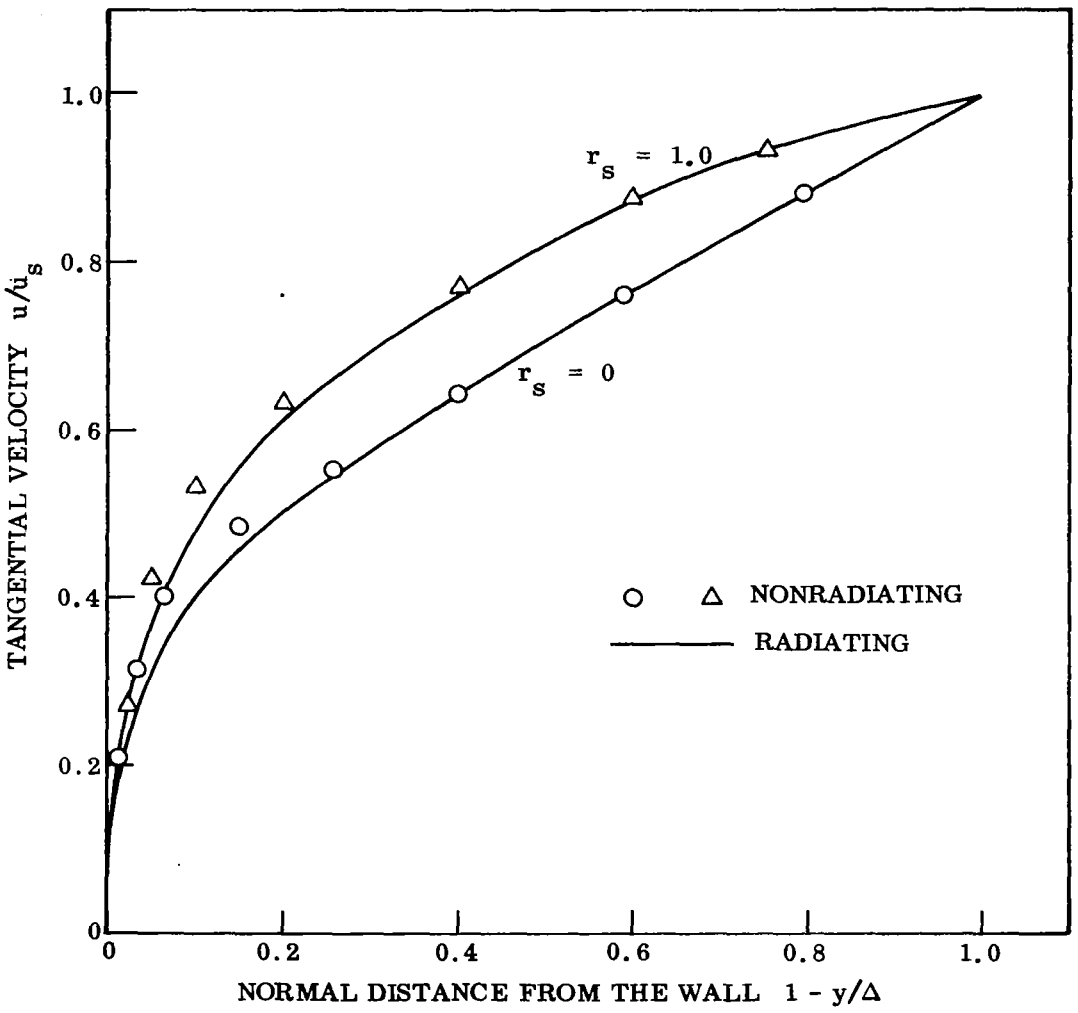

Fig. 12 Viscous Velocity Profile for a Blunted Cone
U_∞ 16 km/cm, $\rho_\infty = 4.21 \times 10^{-7}$ gr/cm^3
R_s = 234 cm

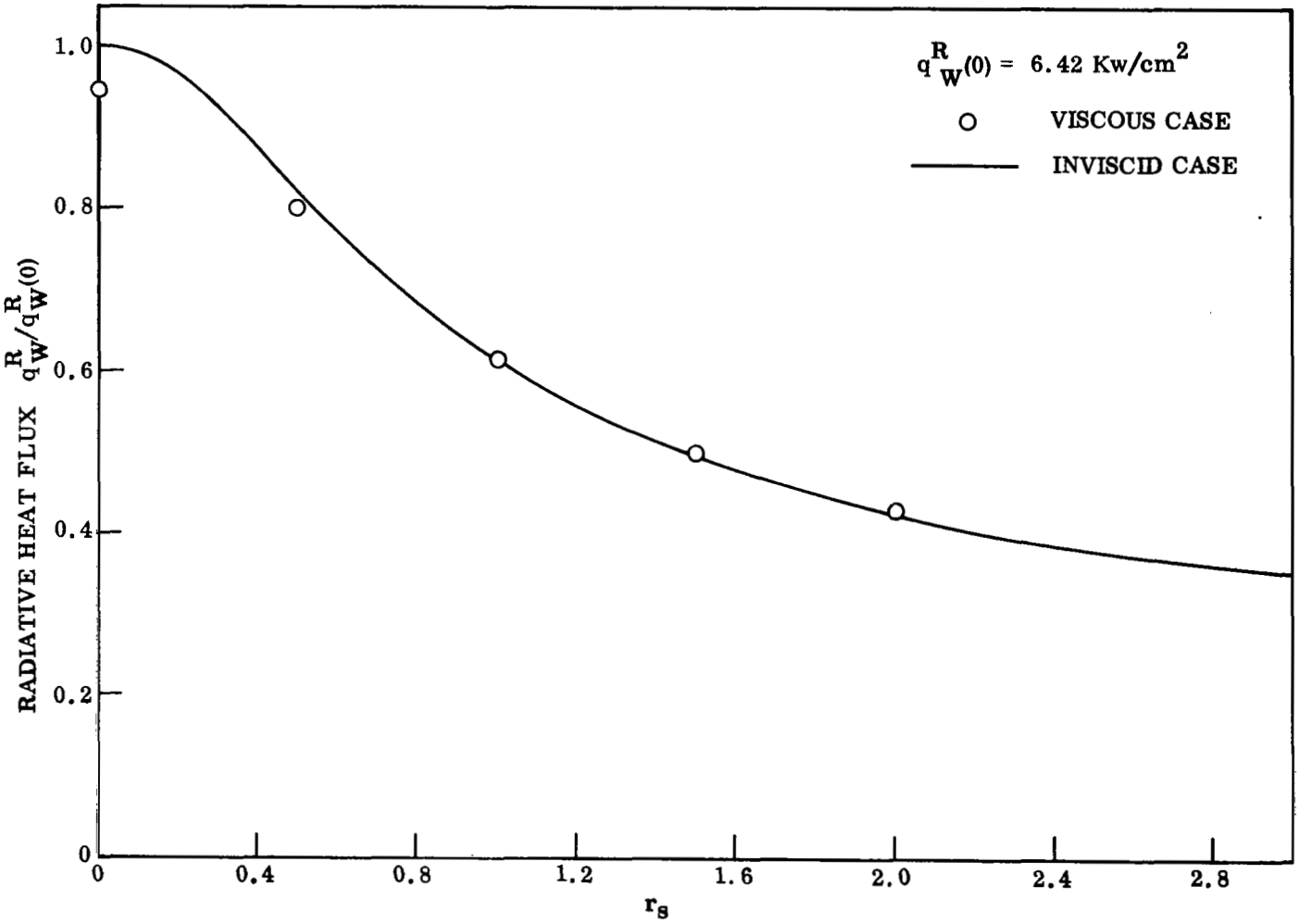

Fig. 13 Radiative Heat Flux Distribution for a Blunted Cone at U_∞ = 16 km/sec, ρ_∞ = 4.21 x 10^{-7} gr/cm^3, R_s = 234 cm

4.3 VISCOUS NONRADIATING CASE WITH SURFACE MASS INJECTION

In order to show the feasibility of the present method in handling a large surface mass injection condition, we have obtained a solution for the case of constant injection rate. The shock shape, the flight conditions, and the transport parameters are the same as given in the last section. However, we have not considered radiative transport for this problem. The only difference is that in the present case $\eta_w = -0.1$ instead of $\eta_w = 0$. This means that at wall there is mass injection at a constant rate of 10% of the freestream mass flow. Note that no diffusion mechanism is allowed in the present formulation. Therefore, the injected gas is assumed to be the same as that of the freestream. The results are presented in Figs. 14 to 16. Results for the nonradiating inviscid and viscous cases are also presented in those figures for comparison. The calculated body shapes are shown in Fig. 14, as one would expect that the effect of the surface mass injection is to increase the shock layer thickness. In the present 10% blowing case, the shock layer thickness increases substantially over the nonblowing cases, especially in the off-stagnation region. In Fig.15, velocity profiles are presented. We see that the viscous layer has been blowing off the wall, and it moves further into the inviscid portion of the shock layer as the flow moves around the body. By comparing the blowing profiles with those from a nonblowing calculation, we see that the velocity gradient at the wall and therefore the skin friction, is reduced substantially by the mass injection. Fig. 16 shows the static enthalpy profiles. Again, by comparing the blowing case with nonblowing case, we see the effect of the blowing is to reduce the convective heat flux at the wall. The effect of blowing on heat flux is more drastic than the effect on skin friction. In the present case, the convective heat flux is reduced to practically zero.

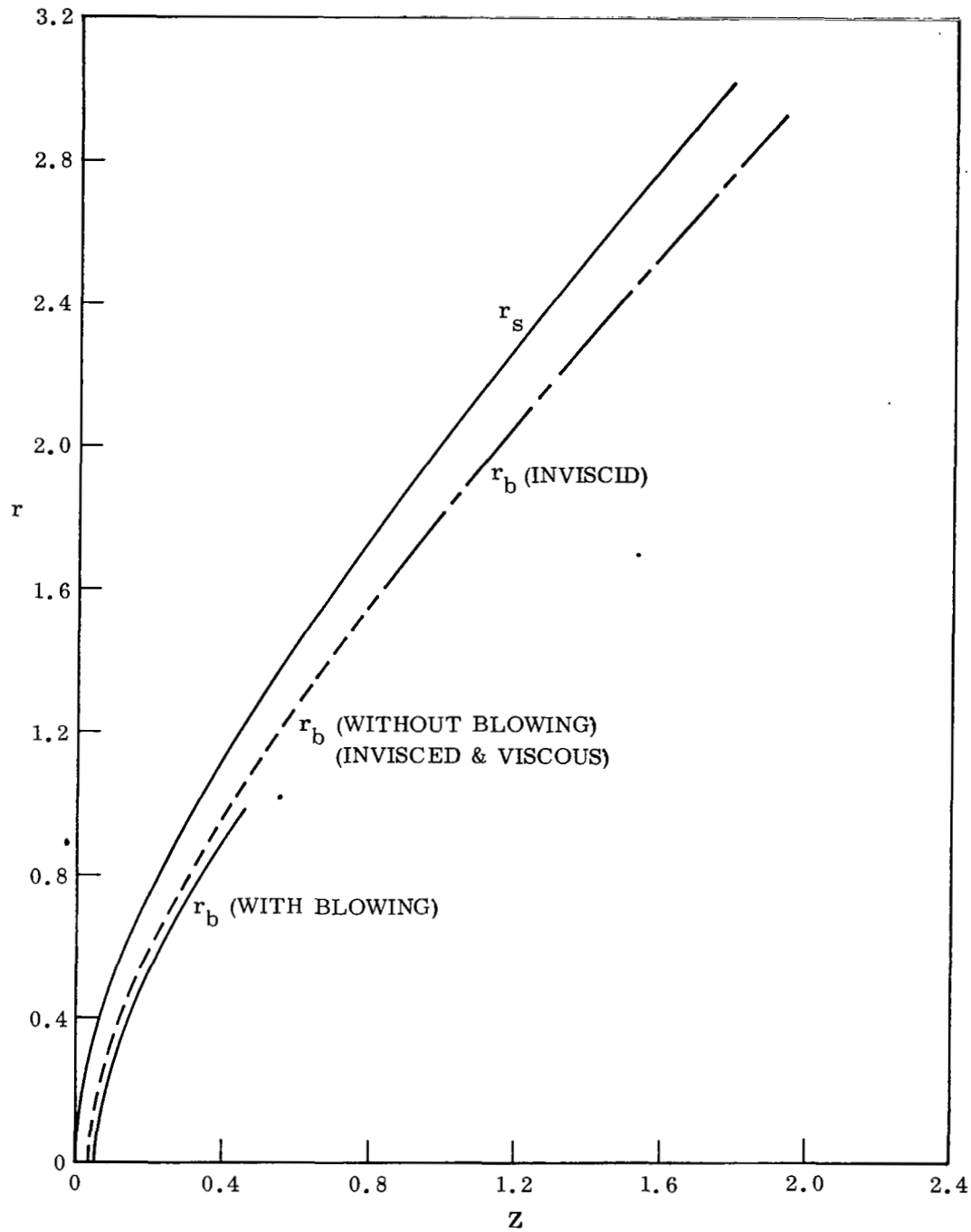

Fig. 14 Shock and Body Shapes for a Blunted Cone with 10% Surface Mass Injection. Adiabatic Case.

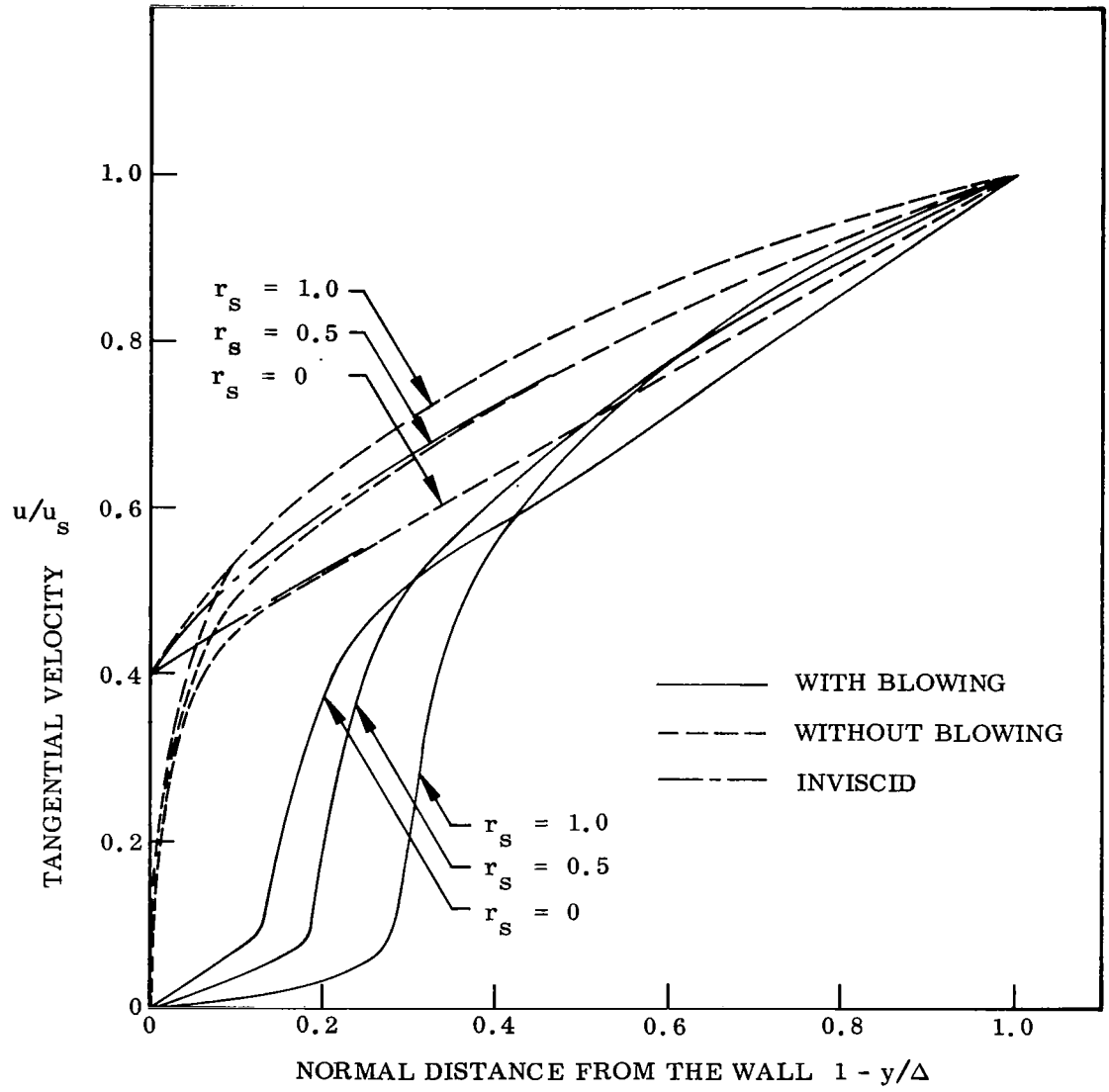

Fig. 15 Velocity Profiles for a Blunted Cone with 10% Surface Mass Injection. Adiabatic Case.

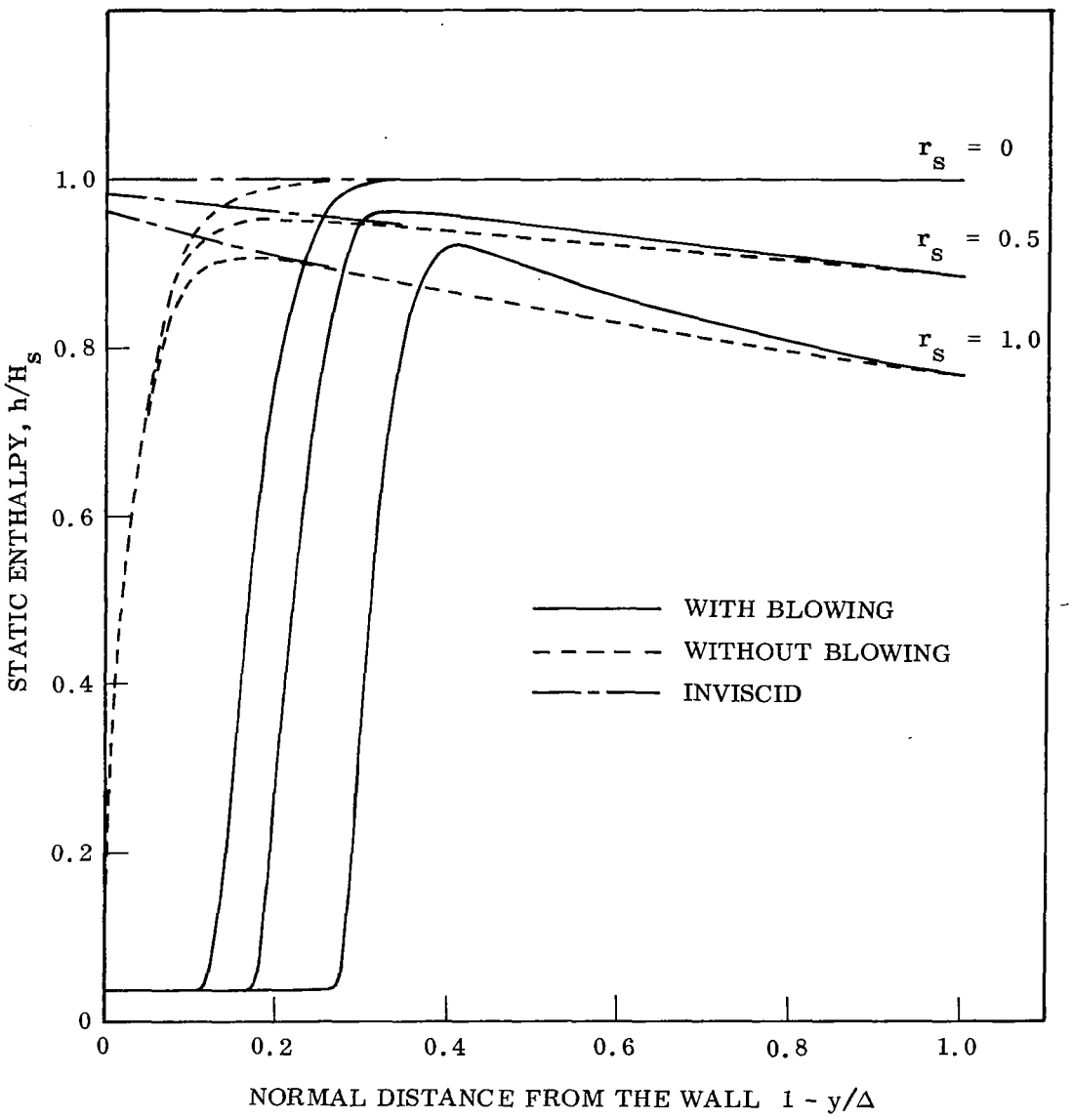

Fig. 16 Adiabatic Static Enthalpy Profiles for a Blunted Cone with 10% Surface Mass Injection

Section 5

CONCLUDING REMARKS

Locally nonsimilar solutions have been obtained for thin shock layers about axisymmetric bodies. Comparisons with existing numerical solutions were made for inviscid nonradiating as well as radiating cases. For viscous cases, due to the lack of available numerical solutions, we have compared our present solutions only with the series solution near the nose region of a blunt body. The agreement in all these comparisons was found to be good. Therefore, the validity of the present solutions have been reasonably demonstrated.

Results are also presented for constant surface mass injection cases. Although no comparison is made (again due to the lack of available numerical solutions) for mass injection cases, the results appear to be physically reasonable. The proper behavior of the solution suggests the applicability of the present method to the mass injection case. It should be noted, however, that slight modifications in the formulation are needed to handle the case of variable injection rates.

Based on the present results, we can draw the following conclusions:
(1) In the case of strong radiative cooling, such as presented in this report, the inviscid shock layer is nearly isothermal at a distance far from the stagnation point; (2) the shock layer thickness grows faster than the boundary layer thickness as the flow flows around the body, therefore the viscous effect decreases, or the relative boundary layer thickness decreases as the flow flows around the body; (3) the radiative flux to the wall is reduced by

less than 10% (for the present flight conditions) at the stagnation point due to viscous cooling. At distances far from stagnation point, the viscous radiative flux to the wall approaches that of inviscid cases; (4) the effect of radiative cooling is mostly thermodynamical rather than fluid dynamical.

Section 6

REFERENCES

1. Y. S. Chou and L. H. Blake, "Thin Radiating Shock Layer About a Blunt Body," NASA CR-1547, March 1970. Also AIAA Journal, Vol. 8, No. 9, Sept. 1970.

2. W. B. Olstad, "Nongrey Radiating Flow About Smooth Symmetric Bodies," AIAA Journal, Vol. 9, No. 1, Jan. 1971.

3. S. H. Maslen, "Inviscid Hypersonic Flow Past Smooth Symmetric Bodies," AIAA Journal, Vol. 2, No. 6, June 1964.

4. E. M. Sparrow, H. Quack and C. J. Boerner, "Local Nonsimilarity Boundary Layer Solution," AIAA Journal, Vol. 8, No. 11, Nov. 1970.

5. K. H. Wilson, "Evaluation of One-Dimensional Approximation for Radiative Transport in Blunt Body Shock Layers," LMSC N-EE-71-3, April 1971.

6. H. T. Ho and R. F. Probstein, "The Compressible Viscous Shock Layer in Rarefied Hypersonic Flow," in Rarefied Gasdynamics, ed. L. Talbot, Academic Press, N. Y., 1961.

7. L. B. Callis, "Coupled Nongray Radiating Flows About Long Blunt Bodies," AIAA J. Vol. 9., No. 4, April 1971.

8. H. K. Cheng and G. A. Gaitatzes, "Use of the Shock-Layer Approximation in the Inverse Hypersonic Blunt Body Problem," AIAA Journal, Vol. 4, No. 3, Mar. 1966.

9. K. H. Wilson, "Stagnation Point Analysis of Coupled Viscous-Radiating Flow with Massive Blowing," NASA CR 1548, June 1970.

APPENDIX I

The Thin Shock Layer Approximation and the Maslen's Approximation at the Stagnation Point

In this appendix, we will show that at the stagnation point, the Maslen approximation is consistent with the thin shock layer approximation. We start with the inviscid ξ and η momentum equations at the stagnation point. They are

$$2\eta f \frac{df}{d\eta} - f^2 = -2\epsilon\left(\eta f - \frac{1}{\xi}\frac{dP}{d\xi}\right) \tag{A1}$$

$$\frac{dP}{d\eta} = \xi^2 f \tag{A2}$$

The notations in Eqs. (A1) and (A2) are the same as that defined in the text. In the case of Maslen's approximation, f is assumed to be equal to unity in the right hand side of both Eq. (A1) and Eq. (A2). Now, by using the relation that at the shock $P_s \tilde{=} 1-u_s^2 = 1 - \xi^2$. Equation (A1) may be written as follows:

$$2\eta f \frac{df}{d\eta} - f^2 = -2\epsilon\left(1+\eta f - \int_{\frac{1}{2}} f d\eta\right) \tag{A3}$$

Equation (A3) under Maslen's approximation is simply

$$2\eta f \frac{df}{d\eta} - f^2 = -3\epsilon \tag{A4}$$

The solution to Eq. (A4) , subject to the boundary conditions: $f = 1$ at $\eta = \frac{1}{2}$, is

$$f = \sqrt{2(1-3\epsilon)\eta+3\epsilon} \tag{A5}$$

We will now show that the solution to Eq. (A3) up to the order of ϵ is identical to Eq. (A5).

Let us differentiate Eq. (A3) with respect to η . We found that the equation is then reduced to

$$\frac{d}{d\eta}\left(f\frac{df}{d\eta}\right) = -\epsilon\frac{df}{d\eta} \tag{A6}$$

Applying the boundary condition at $\eta = \frac{1}{2}$, $f = 1$, and from Eq. (A3), we obtain the condition at $\eta = \frac{1}{2}$, $\frac{df}{d\eta} = 1-3\epsilon$.

Hence, from Eq. (A6), we have

$$f\frac{df}{d\eta} = -\epsilon f + (1-2\epsilon) \tag{A7}$$

Now define a new variable ω , such that

$$\frac{d\eta}{d\omega} = f \tag{A8}$$

and let $\omega = 0$ at $\eta = 0$ and $\omega = \omega_o$ at $\eta = \frac{1}{2}$, where ω_o is yet unknown.

The solution to Eq. (A7) and (A8), subject to the condition that $\eta = 0$, $\omega = 0$ and $\omega = \omega_o$ $f = 1$ is simply

$$f = \frac{1-2\epsilon}{\epsilon} - \frac{1-3\epsilon}{\epsilon}\exp\left(\epsilon(\omega_o-\omega)\right) \tag{A9}$$

$$\eta = \left(\frac{1-2\epsilon}{\epsilon}\right)\omega + \frac{(1-3\epsilon)}{\epsilon^2}\left[\exp\left(\epsilon(\omega_o-\omega)\right) - \exp\left(\epsilon\omega_o\right)\right] \tag{A10}$$

The constant ω_o is to be determined from the condition that $\eta = \frac{1}{2}$ at $\omega = \omega_o$. Thus we have the relation

$$\frac{1}{2} = \left(\frac{1-2\epsilon}{\epsilon}\right)\omega_o + \frac{1-3\epsilon}{\epsilon^2}\left[1 - \exp\left(\epsilon\omega_o\right)\right] \tag{A11}$$

Now, for $\epsilon\omega_o \ll 1$, the exponential term can be expanded and Eq. (A11) becomes

$$\frac{1}{2} = \left(\frac{1-2\epsilon}{\epsilon}\right)\omega_o + \frac{1-3\epsilon}{\epsilon^2}\left[1 - 1 - \epsilon\omega_o - \tfrac{1}{2}\epsilon^2\omega_o^2 - O\left(\epsilon^3\omega_o^3\right)\right]$$

$$\frac{1}{2} = \omega_o\,\frac{1-3\epsilon}{2}\,\omega_o^2\,O(\epsilon\omega_o^3)$$

or,

$$\omega_o \simeq \frac{1}{1+\sqrt{3}\epsilon} \tag{A12}$$

Also, Eq. (A9) and (A10) can be expanded as

$$f = \frac{1-2\epsilon}{\epsilon} - \frac{1-3\epsilon}{\epsilon}\left[1+\epsilon(\omega_o-\omega) + O(\epsilon^2)\right]$$

$$\eta = \left(\frac{1-2\epsilon}{\epsilon}\right)\omega + \frac{1-3\epsilon}{\epsilon^2}\left[1+\epsilon(\omega_o-\omega)-1-\epsilon\omega_o + \tfrac{1}{2}\epsilon^2(\omega_o-\omega)^2 - \frac{\epsilon^2}{2}\omega_o^2 + O(\epsilon^3)\right]$$

After using Eq. (A12), we obtain

$$f = (1-3\epsilon)\omega + \sqrt{3}\epsilon + O(\epsilon) \tag{A13}$$

$$\eta = \tfrac{1}{2}(1-3\epsilon)\omega^2 + \sqrt{3}\epsilon\omega + O(\epsilon\omega^3) \tag{A14}$$

and from Eqs. (A13) and (A14), we arrive at the final result

$$f = \sqrt{2(1-3\epsilon)\eta+3\epsilon} + O(\epsilon) \tag{A15}$$

We see that the solution to Eq. (A3) is identical to the solution to Eq. (A4) up to order of ϵ. Therefore, we conclude that Maslen's approximation is consistent with the thin shock layer approximation.

NASA-Langley, 1972 —— 12